JOC The Journal of Organic Chemistry

ARTICLE

pubs.acs.org/joc

Carba-LNA-^{5Me}C/A/G/T Modified Oligos Show Nucleobase-Specific Modulation of 3′-Exonuclease Activity, Thermodynamic Stability, RNA Selectivity, and RNase H Elicitation: Synthesis and Biochemistry

RamShankar Upadhayaya,[†,§] Sachin Gangadhar Deshpande,[†,§] Qing Li,[‡,§] Ramakant Asaram Kardile,[†] Aftab Yusuf Sayyed,[†] Eknath Kamalakar Kshirsagar,[†] Rahul Vilas Salunke,[†] Shailesh Satish Dixit,[†] Chuanzheng Zhou,[‡] András Földesi,[‡] and Jyoti Chattopadhyaya*[,‡]

[†]Institute of Molecular Medicine, International Biotech Park, Genesis Campus, Phase II Opp Infosys, Tal Mulshi, Hinjewadi, Pune 411 057, India

[‡]Program of Bioorganic Chemistry, Institute of Cell and Molecular Biology, Biomedical Centre, Uppsala University, SE-75123 Uppsala, Sweden

Supporting Information

ABSTRACT:

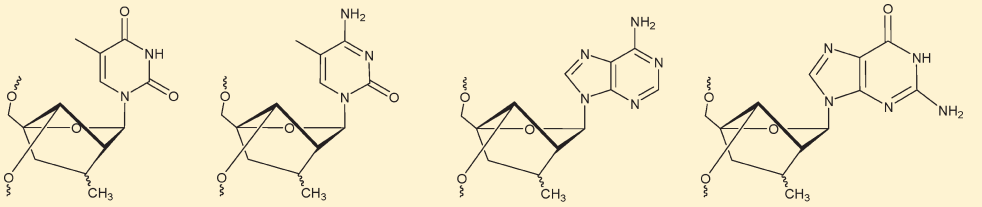

cLNA-T cLNA-^{Me}C cLNA-A cLNA-G

Using the intramolecular 5-*exo*-5-hexenyl radical as a key cyclization step, we previously reported an unambiguous synthesis of carba-LNA thymine (cLNA-T), which we subsequently incorporated in antisense oligonucleotides (AON) and investigated their biochemical properties [*J. Am. Chem. Soc.* **2007**, *129* (26), 8362−8379]. These cLNA-T incorporated oligos showed specific RNA affinity of +3.5−5 °C/modification for AON:RNA heteroduplexes, which is comparable to what is found for those of LNAs (Locked Nucleic Acids). These modified oligos however showed significantly enhanced nuclease stability (ca. 100 times more) in the blood serum compared to those of the LNA modified counterparts without compromising any RNase H recruitment capability. We herein report the synthesis of 5-methylcytosine-1-yl (^{Me}C), 9-adeninyl (A), and 9-guaninyl (G) derivatives of cLNA and their oligonucleotides and report their biochemical properties as potential RNA-directed inhibitors. In a series of isosequential carba-LNA modified AONs, we herein show that all the cLNA modified AONs are found to be RNA-selective, but the magnitude of RNA-selectivity of 7′-*R*-Me-cLNA-G (cLNA-G) (ΔT_m = 2.9 °C/modification) and intractable isomeric mixtures of 7′-(*S*/*R*)-Me-cLNA-T (cLNA-T, ΔT_m = 2.2 °C/modification) was found to be better than diastereomeric mixtures of 7′-(*S*/*R*)-Me-cLNA-^{Me}C with trace of cENA-^{Me}C (cLNA-^{Me}C, ΔT_m = 1.8 °C/modification) and 7′-*R*-Me-cLNA-A (cLNA-A, ΔT_m = 0.9 °C/modification). cLNA-^{Me}C modified AONs however exhibited the best nuclease stability, which is 4-, 7-, and 20-fold better, respectively, than cLNA-T, cLNA-A, and cLNA-G modified counterparts, which in turn was more than 100 times stable than that of the native. When the modification sites are appropriately chosen in the AONs, the cLNA-A, -G, and -^{Me}C modified sites in the AON:RNA hybrids can be easily recognized by RNase H, and the RNA strand of the hybrid is degraded in a specific manner, which is important for the design of oligos for therapeutic purposes. The cLNA-^{Me}C modified AON/RNA, however, has been found to be degraded 4 times faster than cLNA-A and G modified counterparts. By appropriately choosing the carba-LNA modification sites in AON strands, the digestion of AON:RNA can be either totally repressed or be limited to cleavage at specific sites or at a single site only (similar to that of catalytic RNAzyme or DNAzyme). Considering all physico- and biochemical aspects of cLNA modified oligos, the work suggests that the cLNA modified antisense oligos have the potential of being a promising therapeutic candidate due to their (i) higher nucleobase-specific RNA affinity and RNA selectivity, (ii) greatly improved nuclease stability, and (iii) efficient RNase H recruitment capability, which can induce target RNA cleavage in a very specific manner at multiple or at a single site, in a designed manner.

INTRODUCTION

A short oligonucleotide sequence in a single-stranded antisense form (AON) or in a double-stranded form (siRNA) can modulate the gene expression by targeting against the cellular RNA, which is being exploited as potential therapeutics in several laboratories.[1] Several problems in the design of RNA-directed therapeutics are being addressed by different groups including the problem of target affinity, nuclease stability, delivery, and ADME-Tox (Absorption, Distribution, Metabolism, Excretion,

Received: January 12, 2011
Published: April 18, 2011

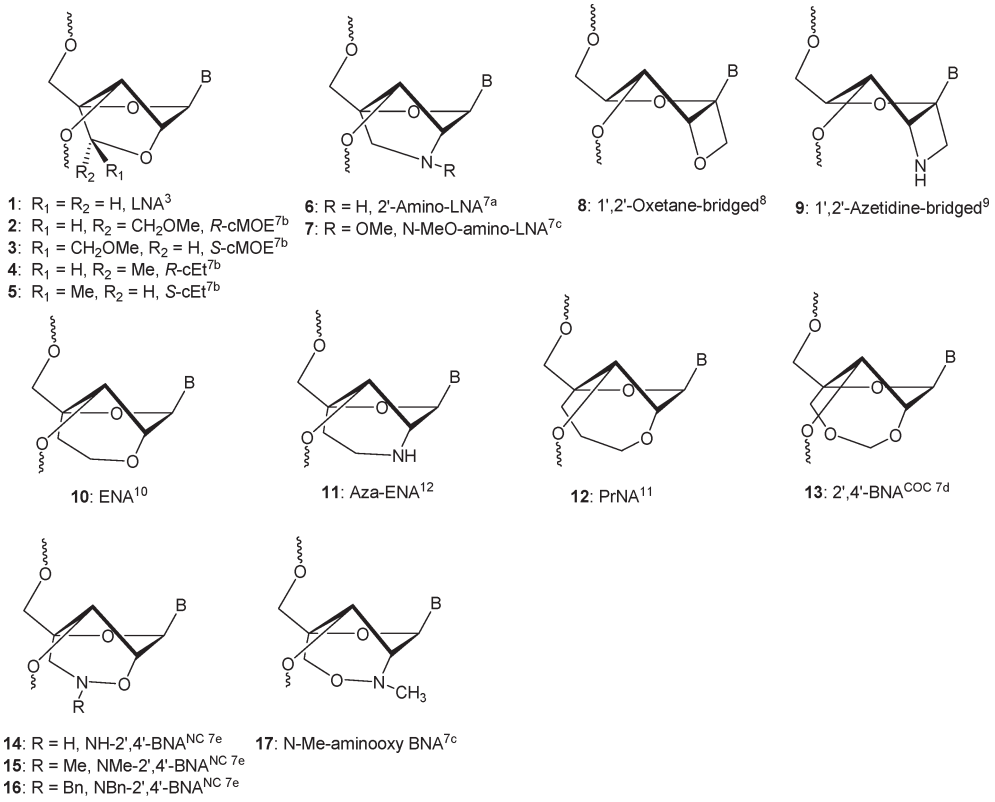

Figure 1. Structures of some representatives of 1′,2′- or 2′,4′-conformationally locked nucleosides.

and Toxicity). Chemical modifications of oligonucleotides have been, however, proved to be an effective strategy to counter some of these problems.[2] Among these, the oligonucleotides modified with LNA (Locked Nucleic Acid, also known as BNA)[3] building blocks have shown several desirable properties, especially their unprecedented affinity toward complementary RNA. The LNA monomer nucleoside blocks have a 2′,4′-bridge [4′-**CH$_2$-O**-2′] locking the sugar conformation in a perfect North-type (*N*-type) conformation [pseudorotation angles, $P \approx 17°$, and the puckering amplitude, $\nu_{max} \approx 56°$].[4] The enhanced target binding property of the North-conformationally constrained bicyclic sugar units in LNA has been attributed to the improved stacking between the nearest neighbors by promoting preorganization of ssLNA owing to restriction of the concerted local backbone motions in the LNA-modified oligos, thereby reducing the entropic penalty for formation of duplex with RNA.[5] These striking conformational features have paved the way for LNA-modified oligos for an extensive application in RNA targeting therapeutics and in biotechnologies.[6]

The intrinsic feature of the North-type sugar constraint in LNA has led to the synthesis of a number of closely related analogues, in which the 2′,4′-bridge has been altered[7] to 2′,4′-BNA^{COC} **13**,[7d] 2′,4′-BNA^{NC} **14**,[7e] 6′-substituted LNAs **2**−**5**,[7b] or a new type of 1′,2′-bridged constraint, such as in the 1′,2′-oxetane **8**[8] or 1′,2′-azetidine **9**[9] analogue (Figure 1). Such modifications show similar or moderately depressed T_m properties when compared to LNA, but the nuclease resistance or RNase H recruitment properties (for example, ENA **10**,[10] PrNA **12**,[11] and aza-ENA **11**[12]) (Figure 1) have turned out to be relatively more favorable than those exhibited by the LNA-containing AONs.

Replacement of the 2′-oxygen of LNA with the 2′-CHR- group leads to carbocyclic locked nucleosides (cLNA and cENA, Figure 2), and the first cENA and its analogues (**18**, **19**, and **23**−**25**, Figure 2) were synthesized by Nielsen's group.[13] These cENA analogues had been incorporated into AONs with a natural phosphodiester backbone, which led to increased thermal stability (T_m) by 2.5−4.5 °C/modification with the complementary RNA.[13] We have recently reported the synthesis[14a] of 7′-Me-carba-LNA-T (cLNA-T) **27** and 8′-Me-carba ENA-T (cENA-T) **22** nucleosides, respectively, involving 5-hexenyl or the 6-heptenyl radical cyclization to a distant double bond tethered at C4′ and the radical center at C2′ of the ribofuranose ring of thymidine. We have demonstrated that cLNA-T enhances the T_m of the modified AON:RNA heteroduplexes by 3.5−5 and 1.5 °C/modification for cLNA-T and cENA-T, respectively. It was also noteworthy that they remarkably enhanced the lifetimes of hydrolysis of these carbocyclic nucleoside-modified AONs in the human blood serum, which may potentially produce the highly desired pharmacokinetic properties because of their unique stability and consequently a net reduction of the required dosage.

This unique quality as well as their efficient use as the AON in the RNase H-promoted cleavage of the target RNA make our cLNA and cENA modifications excellent candidates as potential antisense therapeutic agents.

Later, we continued to fine-tune the electrostatic effects by modulating the chemical character of the 2′,4′-*C*-ethylene bridge (B = 1-thyminyl) by the introduction of a variety of substitutions (H, Me, OH, NH$_2$) at the C6′-positions and the C7′ (or C8′) positions (**28**−**31**) in cLNA and (**20**−**22**) cENA.[14a−g] However, this fine-tuning does not result in major structure variations in

dx.doi.org/10.1021/jo200073q |*J. Org. Chem.* 2011, 76, 4408–4431

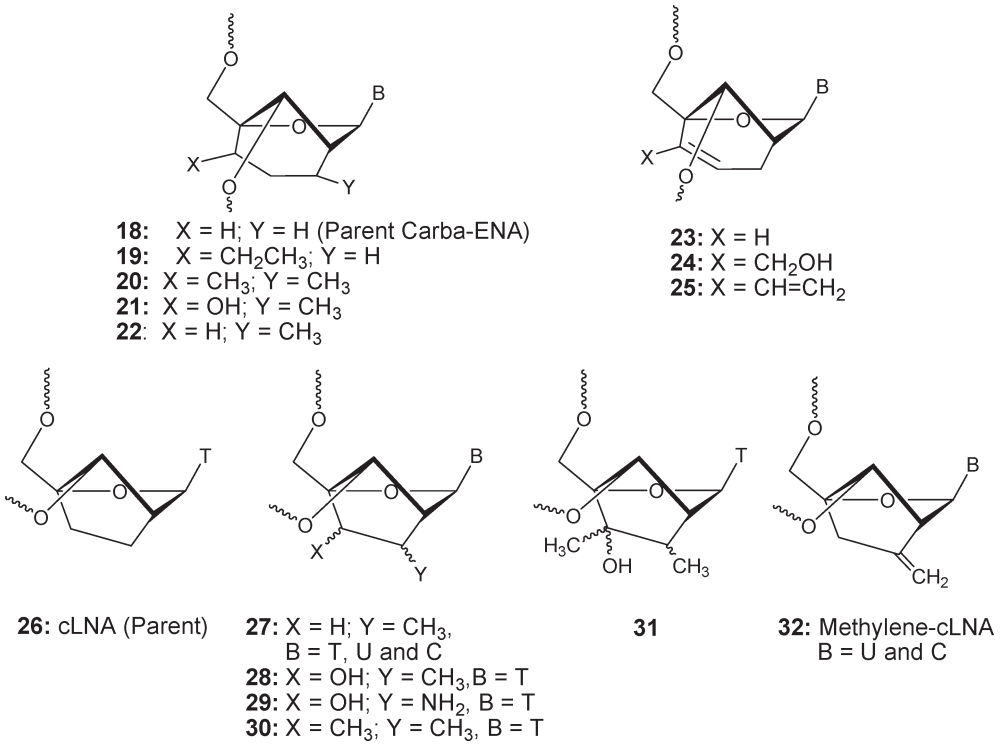

Figure 2. Structures of some known carbocyclic LNA and carbocyclic ENA nucleosides.

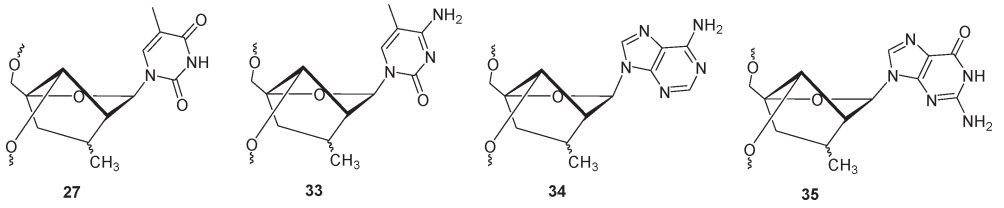

Figure 3. Structures of 2′,4′-constrained cLNA-T/^{Me}C/A/G nucleotides.

terms of recognition of the cDNA and RNA strand, although some of them lead to quite improved nuclease resistance and RNase H recruitment properties relative to cLNA-T **27** and cENA-T **22**.[15]

Recently, Seth and co-workers[14h] have synthesized a few cLNA analogues (methylene-cLNA **32**, see Figure 2), which have 2′,4′-bridged carba skeletons on the pentofuranose ring identical to ours, as in **26**−**31**.[14a−f] This was achieved by the intramolecular free-radical cyclization of the C2′ radical to the C4′-tethered −C≡CH as an extension of our original free-radical cyclization work in which we showed intramolecular addition of the C2′ radical to the C4′-tethered −CH═CH$_2$[14a−c,e,g] or −CH═NOR.[14d,f] It was also found[14h] that oligos with carba-LNA with an exocyclic methylene group at C7′ have T_m values comparable to LNA when hybridized with complementary RNA.

Given the easy accessibility and unique antisense properties of cLNA-T, it was clear that synthesis of cLNA-A/G/^{Me}C derivatives (**33**−**35** in Figure 3) and their oligos should give us a nice opportunity to compare their biophysical and biochemical properties with those of the cLNA-T modified counterparts. We argued that such studies as the relative RNA affinity/selectivity, blood serum stability, and RNase H elicitation capability would give us complete insight into how cLNAs in general could be used as potential antisense or siRNA therapeutic agents. In this paper, we report our results toward this goal by highlighting the unique nucleobase-specific properties among the isosequential cLNA-^{Me}C/T/A/G modified counterparts.

RESULT AND DISCUSSION

1.0. Synthesis of cLNA-A, -G, and -^{Me}C and Their Phosphoramidite Derivatives. *1.1. Synthesis of cLNA-A, -G, and -^{Me}C Nucleosides by the Radical Cyclization Method.* The independent syntheses of cLNA-A (**41a**/**b**), -G (**42a**/**b**), and -^{Me}C (**43a**/**b**/**c**) nucleosides starts from a common starting intermediate **36**[14a] (Scheme 1) which has a C4 tethered propenyl side chain for 5-hexenyl-type free radical cyclization. The compound **36** was subjected to acetolysis using a mixture of acetic anhydride, acetic acid, and triflic acid to give the corresponding diacetate **37** quantitatively as an α/β anomeric mixture. After workup, the crude diacetate **37** was coupled with persilylated protected bases, N^6-benzoyladenine,[16] N^2-acetyl-O^6-diphenylcarbomoylguanine,[17] and N^4-benzoyl-5-methylcytosine,[18] in the presence of Lewis acid TMSOTf to give **38a** (86%), **38b** (60%), and **38c** (80%) in good

dx.doi.org/10.1021/jo200073q |J. Org. Chem. 2011, 76, 4408–4431

Scheme 1[a]

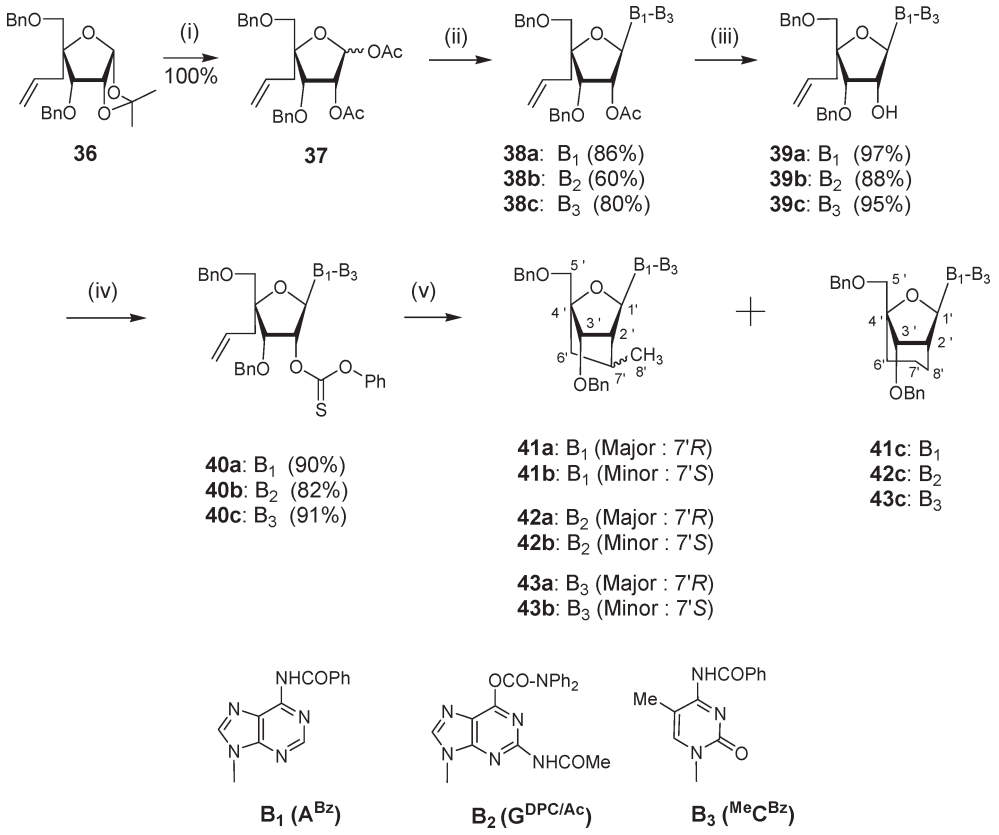

[a] Reagents and Conditions: (i) Ac_2O, AcOH, TfOH, 0 °C to rt, 30 min; (ii) persilylated N^6-benzoyladenine, TMSOTf, CH_3CN, 50 °C overnight for **38a** or (ii) persilylated protected guanine, TMSOTf, toluene, 80 °C, 1.5 h for **38b** or (ii) persilylated N^4-benzoyl-5-Me-cytosine, TMSOTf, CH_3CN, rt, overnight for **38c**; (iii) 2 M NaOH, THF/H_2O, rt, 2 h for **39a** or (iii) 2 M NaOH, THF/H_2O, 0 °C, 2 h for **39b** or (iii) 2 M NaOH, THF/H_2O, rt, 2 h for **39c**; (iv) 1-methylimidazole, phenyl chlorothionoformate, DCM, rt, 5 h for **40a** or (iv) 1-methylimidazole, phenyl chlorothionoformate, DCM, rt, overnight for **40b** or (iv) 1-methylimidazole, phenyl chlorothionoformate, DCM, 1.5 h for **40c**; (v) Bu_3SnH, toluene, AIBN, reflux, 1.5 h; **41a** 38%, **41b** 4%; **41c** 4% or (v) Bu_3SnH, toluene, AIBN, 90 °C, 1.5 h; 48% for **42a**, 4% for **42b**, and 4% for **42c** or (v) Bu_3SnH, toluene, AIBN, reflux, 2.5 h, 60% for **43a**/**b**/**c**.

yields. The separated products **38a**, **38b**, and **38c** have been confirmed to be pure β isomers by 1D-NOE experiments (Supporting Information, Figures SII.16/17, SIII.12/13/14, SIV.16/17).

The 2′-*O*-acetyl groups in compounds **38a**, **38b**, and **38c** were removed using 2 M aqueous NaOH solution in THF/H_2O mixture, yielding nucleosides **39a**, **39b**, and **39c** in 97%, 88%, and 95% yields, respectively. Notably, during this deacetylation step, no side reactions, viz., deprotections at nucleobases, were observed. The key phenoxythiocarbonyl ester derivative at the 2′-*O*-position was synthesized by reaction of the 2′-hydroxy of **39a**, **39b**, and **39c** with phenyl chlorothionoformate and 1-methylimidazole in anhydrous DCM, to form **40a**, **40b**, and **40c** in satisfactory yields (Scheme 1).

The radical cyclization reaction was carried out under reflux in degassed (N_2) anhydrous toluene using Bu_3SnH with radical initiator AIBN, which were added slowly in a dropwise manner to ensure that the radical generated has an adequate lifetime to capture the double bond before it is quenched by hydrogen. The radical cyclization reaction for adenosine **40a** resulted in two spots on the TLC. The higher-R_f spot was major compound **41a** which was characterized as one of the isomers (7′*R*) formed by the 5-*exo* cyclization reaction, and the lower-R_f spot was found to be a mixture of the second isomer (7′*S*) of the 5-*exo* cyclization product **41b** and 6′-*endo* cyclization product **41c**,[14b] which were separated by preparative HPLC. The isolated yields were 38, 4, and 3.9% for the major isomer **41a** (7′*R*), the minor isomer **41b** (7′*S*), and the 6-*endo* product **41c**, respectively. Similarly, radical-mediated cyclization of guanosine **40b** gave two 5-*exo* cyclization products **42a** (7′*R*, 48%) and **42b** (7′*S*, 4%) and one 6′-*endo* cyclization product **42c** (4%). Cyclization of 5-methylcytosine derivative **40c** generated 5-*exo* cyclization products **43a** and **43b** and 6′-*endo* cyclization product **43c** as a mixture (overall yield 60%) in a ratio of 79:12:9 by NMR. For unequivocal characterization of the reaction products, this mixture was separated by HPLC to give analytical samples of **43a**, **43b**, and **43c** (see Supporting Information, SI General methods).

It is known that cyclization of 5-hexenyl-1-radical is a kinetically controlled process and generally prefers the *exo* cyclization product (*exo*/*endo* > 98/2).[19] In the present study, treatment of the radical precursor **40a**, **40b**, or **40c** with Bu_3SnH and AIBN in refluxing toluene gave C2′ carbon radical intermediates TS I, TS II, and TS III, respectively (Figure 4), followed by intramolecular addition of the C2′ radical to the tethered C═C, giving 5-*exo* cyclization products (~92%) plus ~8% of 6-*endo* cyclization products. We previously reported that radical cyclization of the

dx.doi.org/10.1021/jo200073q |*J. Org. Chem.* 2011, 76, 4408–4431

thymine counterpart also furnished 5-*exo* and 6-*endo* products in a ratio of 92:8.[14b] Hence, it seems no matter what nucleobase is at the anomeric center, cyclization of 5-hexenyl-1-radical in these nucleoside systems generates a slightly increased 6-*endo* product compared with normal cases (8% versus 2%).

1.2. Structural Evidence from NMR for cLNA-A, -G, and -^{Me}C Nucleosides As Well As 6-endo Cyclization Products. cLNA nucleosides **41a/b**, **42a/b**, and **43a/b** and 6-*endo* cyclization products carbocyclic ENA nucleosides **41c**, **42c** and **43c** have been unambiguously characterized using 1D and 2D NMR including ^{1}H, ^{13}C, DEPT, as well as NOE, COSY, ^{1}H−^{13}C HMQC, and long-range ^{1}H−^{13}C correlation (HMBC) experiments.

The formation of the C2′−C7′ bond in cLNA nucleosides **41a/b**, **42a/b**, and **43a/b** has been confirmed unequivocally: first, by the presence of correlation between H2′ and H7′ in

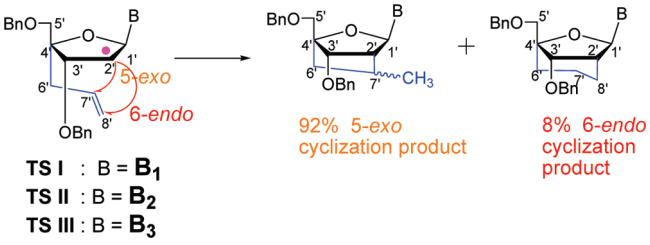

Figure 4. 5-Hexenyl-1-radical cyclization through competing 5-*exo* versus 6-*endo* pathway.

COSY spectra (Figure 5), and second, by the observable $^{3}J_{HC}$ HMBC correlation between H1′ and C7′, H2′ and C6′, and $^{2}J_{HC}$ HMBC correlation between H7′ and C2′ (Figure 6). These proton−proton connectivities in the COSY and proton to carbon connectivities in HMBC proved that the oxa-bicyclo-[2.2.1]heptane ring systems in cLNA-A, -G, and -^{Me}C nucleosides have indeed been formed during the radical cyclization.

The configuration of C1′ and C7′ centers in cLNA nucleosides **41a/b**, **42a/b**, and **43a/b** has been determined by 1D NOE experiments (see Supporting Information Figure SII 65−66, 86−87, SIII 48−51, 68−69, SIV 72−73, 91−92). For **41a**, irradiation of H3′ led to 3% of NOE enhancement for H8, suggesting that the 9-adeninyl moiety is in β configuration and in an *anti* conformation across the glycoside bond. The fact that the NOE enhancement of 2.9% for H1′ upon irradiation on 7′-CH_3 has been observed indicates that the methyl group on C7′ is in close proximity of H1′ ($d_{H1',7'Me} \approx 2.1$ Å) in **41a**, thereby confirming the *R*-configuration at the C7′ center (Figure 7). On the other hand, in the minor product **41b**, irradiation of H1′ led to 5.5% NOE enhancement for H7′ ($d_{H1',H7'} \approx 2.1$ Å) but none for 7′-Me ($d_{H1',7'Me} \approx 3.8$ Å). Hence, the stereochemistry at C7′ has been assigned to *S* configuration in compound **41b**. In a similar way, the C7′ of the major cyclization products **42a** and **43a** has been assigned to *R*-configuration, and the minor products **42b** and **43b** to C7′-*S* configuration (Figure 7).

For the 6-*endo* cyclization product **41c**, the ring closure by formation of the C2′−C8′ bond has been unequivocally confirmed by the following NMR observations: (1) $^{3}J_{HH}$

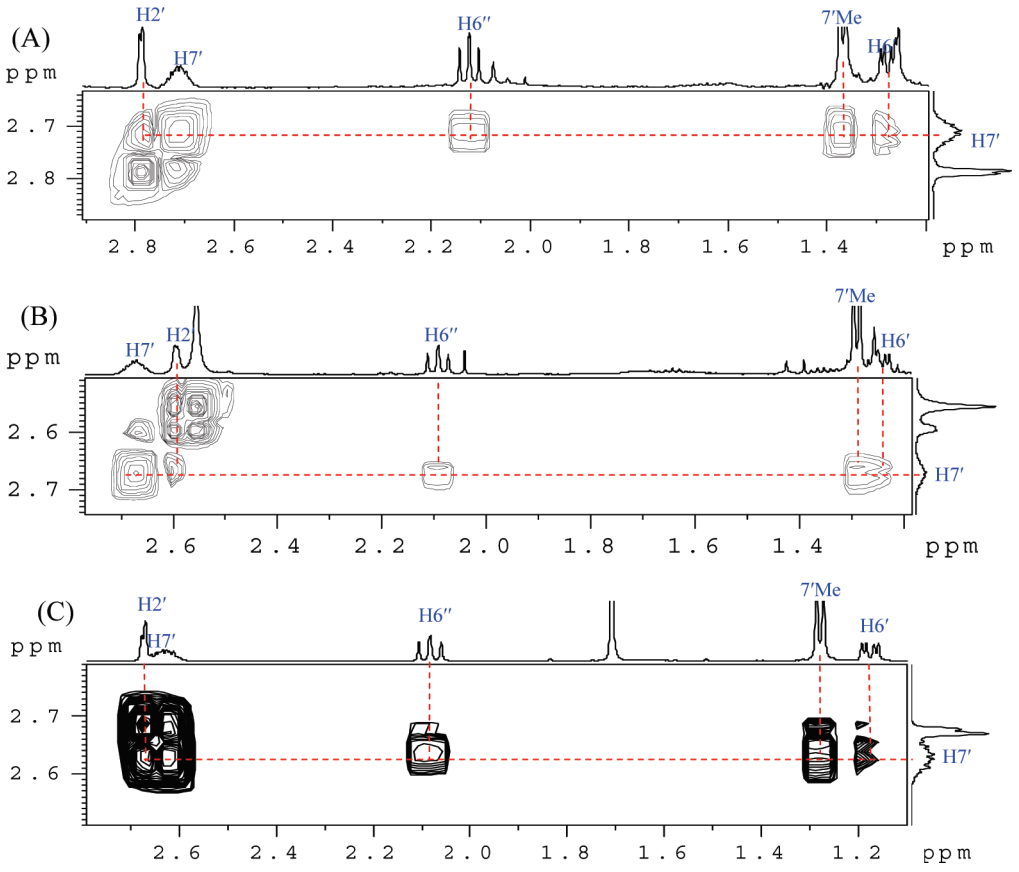

Figure 5. COSY spectra of compounds' major 5-*exo* products **41a** (panel A), **42a** (panel B), and **43a** (panel C). The correlations between H7′ and H2′ indicate that the C2′−C7′ bonds have been formed in these compounds.

dx.doi.org/10.1021/jo200073q |*J. Org. Chem.* 2011, 76, 4408–4431

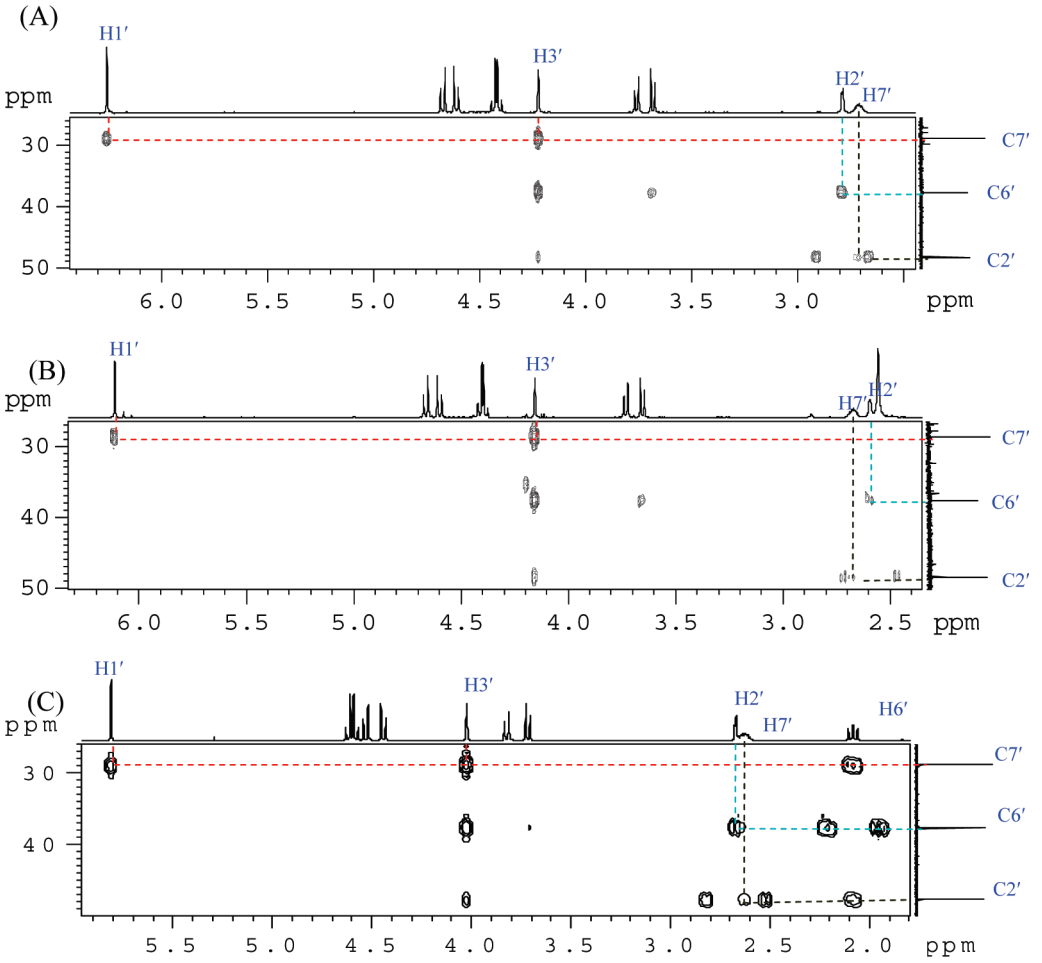

Figure 6. HMBC spectra of compounds **41a** (panel A), **42a** (panel B), and **43a** (panel C). The correlations between H1′ and C7′ (indicated by red dashed lines), H3′ and C7′ (indicated by red dashed lines), H2′ and C6′ (indicated by turquoise dashed lines), and H7′ with C2′ (indicated by black dashed lines) indicate that the C2′−C7′ bonds have been formed in these compounds.

correlation between H8′ and H2′ in the COSY spectrum (Figure 8A); (2) $^{3}J_{HC}$ HMBC correlations between H1′ and C8′ (Figure 8C); (3) DEPT (Supporting Information, Figure SII.98) and HMQC (Figure 8B) spectra showed that both C7′ and C8′ are secondary carbons, each of them having two protons attached. Similar NMR experiments have also been carried out to prove that the oxa-bicyclo[3.2.1]octane ring system has been formed for compounds **42c** (Figure 8D−F) and **43c** (Figure 8G−J).

1.3. Synthesis of Phosphoramidites of cLNA-A, -G, and -^{Me}C. To transform the cLNA-A^{Bz} nucleoside to the corresponding phosphoramidites, the major isomer **41a** was subjected to 3′,5′-debenzylation, using the $Pd(OH)_2$/ammonium formate procedure.[14a] This reaction led to desired debenzylated compound **45a** which was however contaminated with N-debenzoylated product **44a**. To avoid formation of any N-alkylated product later on, we decided to deprotect the N^6-benzoyl group of **41a** before 3′,5′-debenzylation (Scheme 2A). Thus, treatment of **41a** with methanolic ammonia at rt for 16 h furnished N^6-debenzoylated compound **41a**′, which was then subjected to classical 20% $Pd(OH)_2$/C, ammonium formate procedure, giving debenzylated nucleoside **44a** in moderate yield. Following Jones′ transient protection method,[20] the nucleoside **44a** was treated with TMS-Cl in dry pyridine and followed by in situ addition of benzoyl chloride. Subsequently, treatment with aqueous ammonia furnished the desired the 3′,5′-debenzylated cLNA-A^{Bz} (**45a**). The overall yield of this conversion from **41a** to **45a** in three steps was 35% (Scheme 2A). 3′,5′-Debenzylated cLNA-^{Me}C^{Bz} (**47a/b/c**) as a mixture was also obtained in moderate yield starting from **43a/b/c** by a similar strategy (Scheme 2C). It should be noted that we have, however, separated and characterized each component of the mixture of **43a/b/c** (79:12:9 by NMR) in a small scale (see the Experimental Section). This separation, however, did not work in our hands at a larger scale required for the preparation of the corresponding phosphoramidites (required 4−5 steps, Scheme 2). Hence, we proceeded with the mixture of **43a/b/c** to make the phosphoramidites **51a/b/c** as described in Scheme 2 (**43a/b/c** →**47a/b/c** → **50a/b/c** → **51a/b/c**).

For the transformation of guanine derivative **42a** to phosphoramidites, it was critically important to selectively remove the bulky O^6-diphenylcarbamoyl group first. The basic conditions such as aqueous NaOH, methanolic NH_3,[21] or fluoride ion[22] only led to a mixture of desired and undesired products. Another strategy for this purpose is full deprotection followed by selective reprotection of N2, but it was laborious and time-consuming. We have also tried to treat **42a** with 90% trifluoroacetic acid;[23] however, only 25−30% of the desired compound **42a**′ was

dx.doi.org/10.1021/jo200073q |*J. Org. Chem.* 2011, 76, 4408–4431

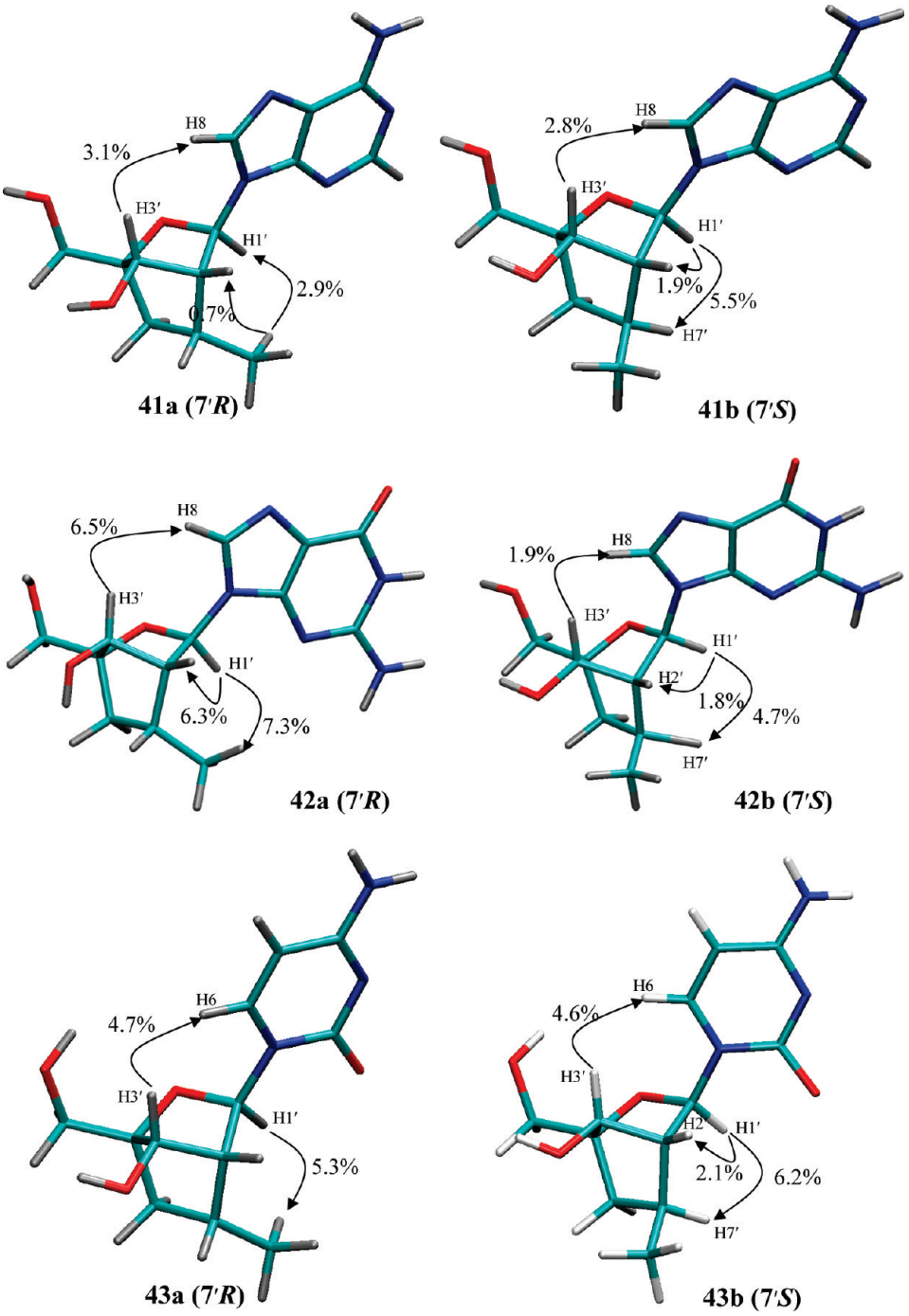

Figure 7. NOE contacts in compounds **41a/b**, **42a/b**, and **43a/b**. In **41a**, **42a**, and **43a**, the observation of NOE enhancement between H1′ and 7′-Me and complete absence of NOE between H1′ and H7′ suggest the C7′-*R* configuration. The reverse observation in compounds **41b**, **42b**, and **43b** indicates the C7′-*S* configuration for them. The β orientation and *anti* conformation across the glycoside bond of the base moieties for all of these compounds can be confirmed by the strong NOE between H3′ and H6 or H8 of nucleobases.

obtained, and the rest was a mixture of polar deglycosylated products. However, a treatment with glacial acetic acid under moderately warm conditions, followed by RT stirring, was found successful, giving the desired O^6-deprotected nucleoside **42a′** in 60−62% yields. Debenzylation of **42a′** using the classical Pd-$(OH)_2$/ammonium formate method furnished only N^2-deacetylated product, and 3′,5′-dibenzyl groups were completely intact. Fortunately, use of formic acid as a hydride source instead of ammonium formate was found to be helpful.[24] Thus, **42a′** was debenzylated using 20% $Pd(OH)_2/C$ and formic acid in dry methanol, yielding the desired diol **45b** in 60% yield (Scheme 2B).

The 5′-primary hydroxyl group in **45a**, **45b**, and **47a/b/c** was selectively protected by DMTr according to a standard procedure,[14a] yielding **48a**, **48b**, and **50a/b/c**, respectively. Phosphitylation of **48a**, **48b**, and **50a/b/c** was first tried using

dx.doi.org/10.1021/jo200073q |*J. Org. Chem.* 2011, 76, 4408–4431

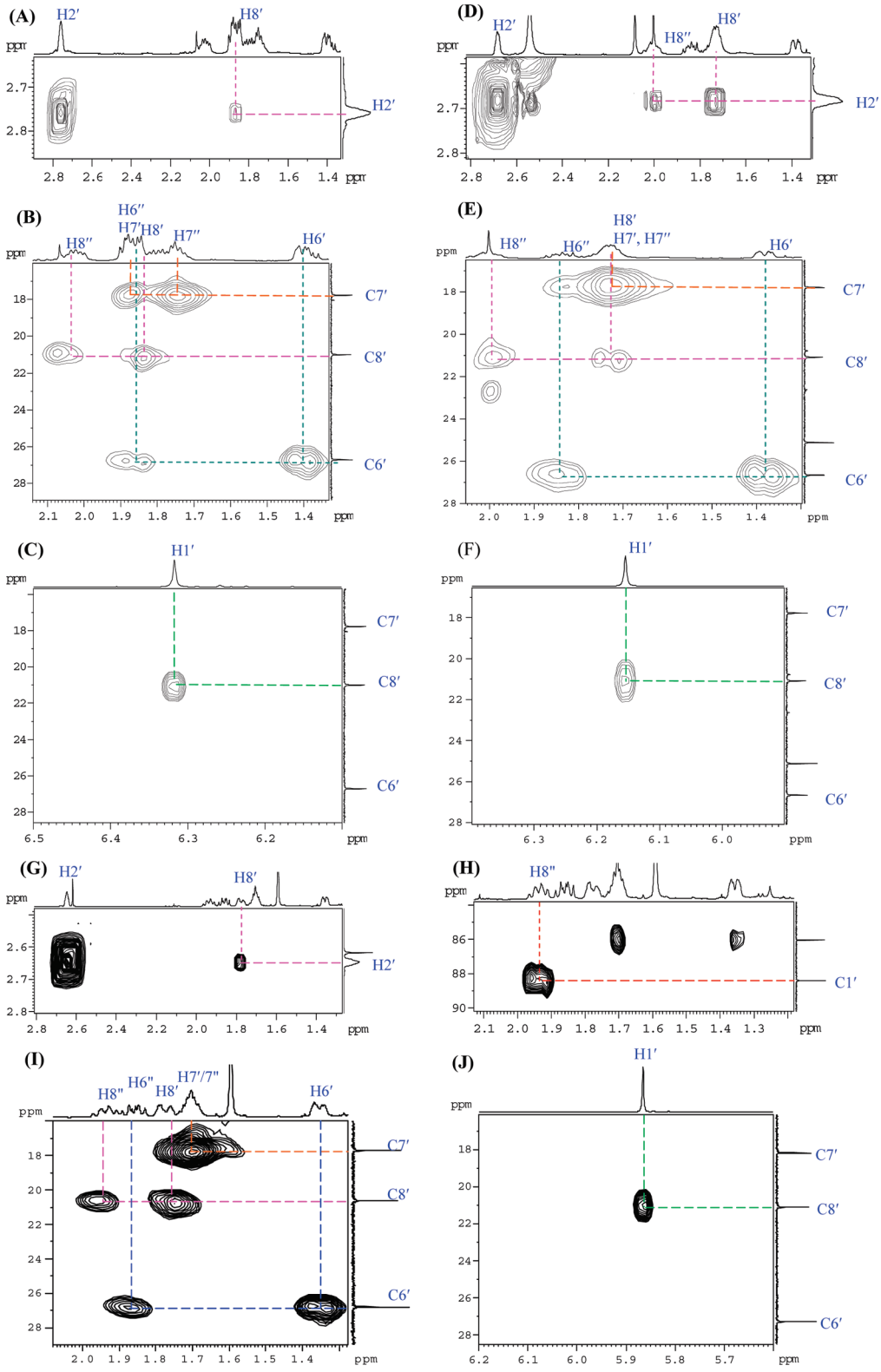

Figure 8. COSY, HMQC, and HMBC spectra of compounds **41c** (panels A–C), **42c** (panels D–F), and **43c** (panels G–J). The $^{3}J_{HH}$ correlation between H8′ and H2′ in COSY spectra (panels A, D, and G, indicated by pink dashed lines) and $^{3}J_{HC}$ HMBC correlations between H1′ and C8′ (panels C, F, and J, indicated by green dashed lines) and H8″ and C1′ (panel H, indicated by red dashed lines) suggest that the oxa-bicyclo[3.2.1]octane ring system has been formed for compounds **41c**, **42c**, and **43c**, which can be further confirmed by HMQC (panels B, E, and I) spectra, showing both C7′ and C8′ have two protons (correlations are indicated by pink dashed lines for C8′ with H8′ and H8″, indicated by orange dashed lines for C7′ with H7′ and H7″) attached.

dx.doi.org/10.1021/jo200073q |*J. Org. Chem.* 2011, 76, 4408–4431

Scheme 2[a]

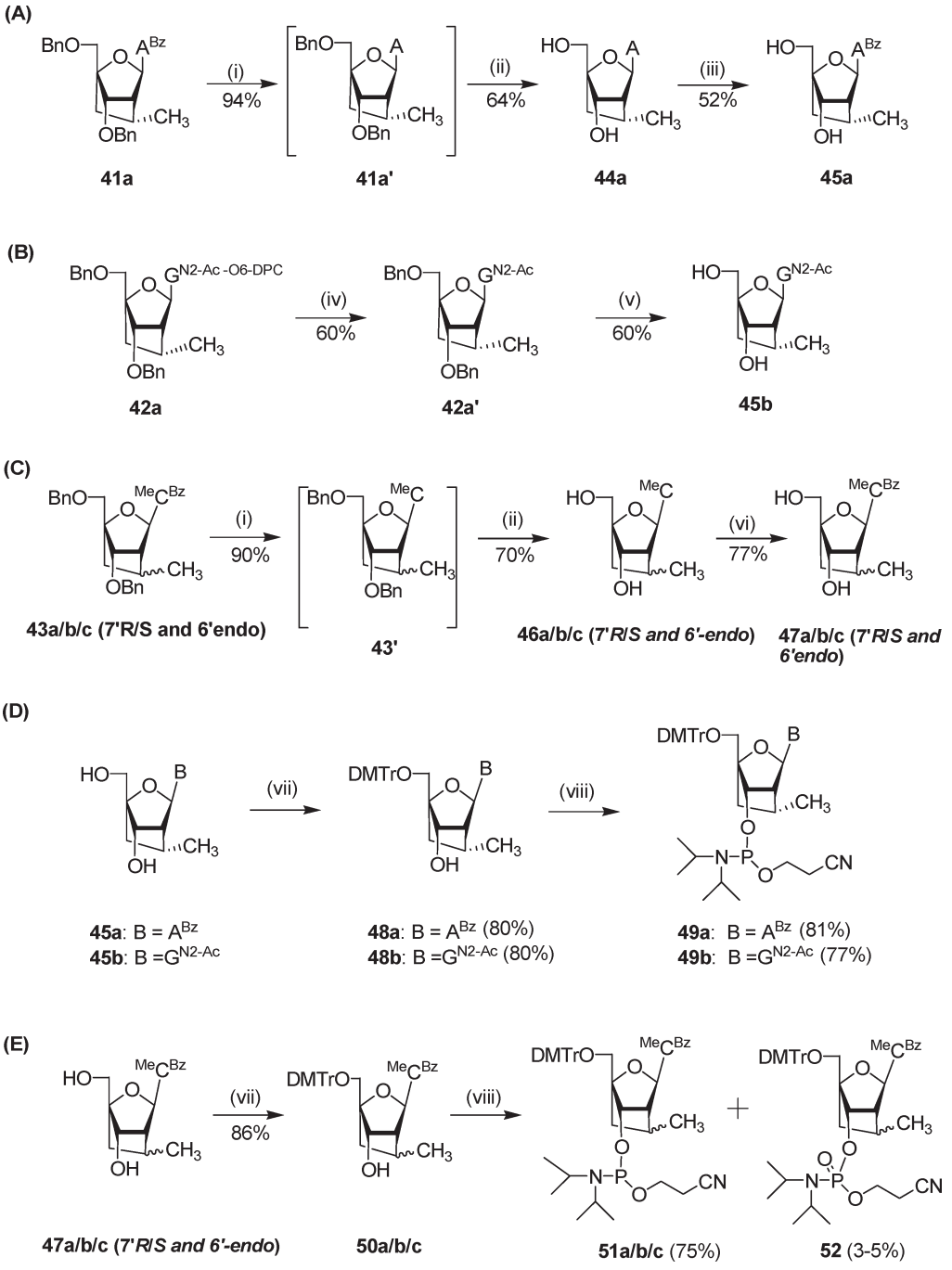

[a] Reagents and conditions: (i) methanolic ammonia, rt, 16 h; (ii) 20% $Pd(OH)_2/C$, ammonium formate, methanol, reflux, 16 h; (iii) a. TMSCl, dry pyridine; b. BzCl, c. aq NH_3; (iv) acetic acid, 55 °C; (v) 20% $Pd(OH)_2/C$, formic acid, methanol, reflux, 2.5 h; (vi) Bz_2O, pyridine, rt, overnight; (vii) DMTrCl, pyridine, rt, overnight; (viii) 2-cyanoethyl-*N*,*N*-diisopropylphosphoramidochloridite, DIPEA, dry DCM, rt, 2 h.

standard conditions,[14a] 2 equiv of 2-cyanoethyl *N*,*N*-diisopropylphosphoramidochloridite in the presence of DIPEA with anhydrous and radical free THF as solvent, rt, overnight under the inert N_2 environment. However, this methodology led to a consistent polar impurity in invariable amount along with desired phosphoramidite products **49a**, **49b**, and **51a/b/c**. These polar impurities show mass equal to M + 16 and were inseparable by column chromatography and various means of precipitations and washings. The polar contamination for the ^{Me}C derivative **51a/b/c** was found more pronounced. ^{31}P NMR of a crude reaction mixture of **51a/b/c** showed six peaks at δ 150.20, 150.04, 149.46, 149.22, 148.94, and 148.80 and additional signals between δ 7.0 and 8.4. The upfield shift in ^{31}P NMR spectra and the mass analysis suggest the polar impurities are oxidized phosphate P(V) derivatives.[25,26]

Clearly, to circumvent the oxidation problem in the phosphitylation reaction, use of (oxygen-free) nonpolar solvents and the reduction of reaction time as well as lesser exposure of reaction

dx.doi.org/10.1021/jo200073q |*J. Org. Chem.* 2011, 76, 4408–4431

Table 1. T_m Values of Duplexes Formed by Modified AONs with Complementary RNA and DNA[a]

oligo name	sequence of AONs	T_m of AON/RNA	ΔT_m/mod of AON/RNA[b]	T_m of AON/DNA	ΔT_m/mod of AON/DNA[c]	ΔT_m[d]
AON **1**	5′ TCC CGC CTG TGA CAT GCA TT	74.0 °C	0 °C	71.0 °C	0 °C	+3.0 °C
AON **2**	5′ TCC CGC CTG TGA CAT GCA TT	77.5 °C	+1.2 °C	74.7 °C	+1.2 °C	+2.8 °C
AON **3**	5′ TCC CGC CTG TGA CAT GCA TT	80.0 °C	+2.0 °C	71.2 °C	+0.1 °C	+8.8 °C
AON **4**	5′ TCC CGC CTG TGA CAT GCA TT	82.0 °C	+2.7 °C	76.7 °C	+1.9 °C	+5.3 °C
AON **5**	5′ TCC CGC CTG TGA CAT GCA TT	83.0 °C	+3.0 °C	76.4 °C	+1.8 °C	+6.6 °C
AON **6**	5′ TCC CGC CTG TGA CAT GCA TT	78.0 °C	+1.3 °C	72.4 °C	+0.5 °C	+5.6 °C
AON **7**	5′ TCC CGC CTG TGA CAT GCA TT	79.0 °C	+1.7 °C	72.8 °C	+0.6 °C	+6.2 °C
AON **8**	5′ TCC CGC CTG TGA CAT GCA TT	87.5 °C	+4.5 °C	76.3 °C	+1.8 °C	+11.2 °C

[a] T_m values measured at the maximum of the first derivative of the melting curve ($A_{260\ nm}$ vs temperature) in medium salt buffer (60 mM tris-HCl at pH 7.5, 60 mM KCl, 0.8 mM $MgCl_2$) with temperature 20−90 °C using 1 μM concentrations of two complementary strands. The values of T_m given are averages of three independent measurements (the error of the three consecutive measurements is within ±0.3 °C). A = cLNA-A; G = cLNA-G; C = cLNA-^{Me}C; T = cLNA-T. [b] ΔT_m of AON/RNA/mod was obtained by comparing the T_m of AON/RNA with that of the native AON **1**/RNA. [c] ΔT_m of AON/DNA/mod was obtained by comparing the T_m of AON/DNA with that of the native AON **1**/DNA. [d] RNA selectivity: ΔT_m = (T_m of AON/RNA) − (T_m of AON/DNA). See footnote under ref 31 for why the AON−RNA duplex is more stable than the AON−DNA counterpart.

mixture to the environmental conditions were inevitable conditions to follow. Thus, modified phosphitylation reactions were carried out in dry DCM (dried over P_2O_5), using 2 equiv of 2-cyanoethyl *N*,*N*-diisopropylphosphoramidochloridite in the presence of DIPEA for invariably 2−2.5 h of reaction time. Phosphoramidites **49a**, **49b**, and **51a/b/c** were obtained in 81%, 77%, and 75% yield, respectively. However, under this condition, ^{Me}C-phosphoramidites **51a/b/c** were found still contaminated by 3−5% of P(V) impurity **52**, which was hard to be removed. Given the nature of the P(V) impurity that is relatively inert compared to active P(III) phosphoramidite, 3−5% of this impurity has not proven to be harmful for the oligomer synthesis in purity and yield. Hence, we did not invest further efforts for purification of **51a/b/c**.

2.0. Thermal Denaturation Studies. The modified phosphoramidites **49a** and **49b** and a mixture of **51a/b/c** were incorporated into a 20mer AON through the solid phase synthesis protocol[27] on an automated DNA/RNA synthesizer. The sequences of AONs and T_m values of duplexes formed by these AONs with complementary RNA and DNA are listed in Table 1.

2.1. cLNA-T, A, G, and ^{Me}C Modifications in AON Strands Lead to Different T_m Increase for AON/RNA Hybrids. Just like cLNA-T, cLNA-A, -G, and -^{Me}C modifications in the same AON sequence also led to T_m increase for the AON:RNA duplex, but the ΔT_m varied significantly with different base types. Triple cLNA-A, triple cLNA-G, triple cLNA-^{Me}C, and triple cLNA-T modification in the AON sequence resulted in a 3.5, 6, 8, and 9 °C increase, respectively. Hence, their RNA affinities decrease in the following rank: cLNA-T (+3.0 °C/modification) > cLNA-^{Me}C (+2.7 °C/modification) > cLNA-G (+2.0 °C/modification) > cLNA-A (+1.2 °C/modification). It seems that pyrimidine-type cLNAs show higher RNA affinity than purine-type counterparts, which is in contrast to 1′,2′-oxetane modification.[8] Therefore, introduction of pyrimidine-type cLNA modification in the oligos is preferable for the design of the antisense strand in the antisense approach. This presumably suggests that the relative strength of cLNA-modified-AON:RNA base pairing versus oxetane-modified-AON:RNA base pairing is dictated by the choice of modification site as well as by the type of chemical modification employed because the relative stability of the duplex is dictated by the combined strength of stacking and base pairing ability in each strand which are different depending upon the sequence context.

For AONs containing both cLNA-A and cLNA-G modifications such as AON **6** and **7**, T_m rise also followed 1 °C/cLNA-A modification and 2 °C/cLNA-G modification. Interestingly, the T_m of AON **8**/RNA was found to be 13.5 °C higher than the native counterpart, which is much higher than expectation given that AON **8** contains three cLNA-A and three cLNA-G modifications. This observation indicates that cLNA-A and cLNA-G modification can lead to a much more pronounced T_m rise in the AON sequence with multiple modifications.

2.2. cLNA-T, A, -G, and -^{Me}C Modified AONs Are RNA-Selective, But the Magnitudes of RNA Selectivity Are Different. All the T_m values of cLNA modified AON **2**−**8**/DNA are higher than that of native AON **1**/DNA, suggesting that cLNA modifications in the AON strand may also result in increased affinity toward cDNA compared to the native type, while these results were found to be different from the T_m results obtained in our lab,[14a] in which we have shown that cLNA-T (isomeric mixture of 7′-*R*/*S*-Me) modified oligos lead to a small decrease in thermodynamic stability with cDNA compared to the native type. This is most probably due to the different sequences (15mer[14a] versus 20mer in this paper) and modification numbers and sites employed here, which caused a positive effect on the stability of cLNA-T modified AON/DNA duplexes versus the native AON/DNA duplex. However, we found for all of the modified AON strands that the T_m of AON/DNA is lower than the T_m of AON/RNA, indicating cLNA modified AONs are RNA-selective (see footnote under ref 32 for why the AON−RNA duplex is more stable than the AON−DNA counterpart). The magnitude of RNA-selectivity, ΔT_m (ΔT_m = [T_m of AON/RNA] − [T_m of AON/DNA]), was found to be 2.8, 8.8, 5.3, and 6.6 °C, respectively, for triple cLNA-A modified AON **2**, triple cLNA-G modified AON **3**, triple cLNA-C modified AON **4**, and triple cLNA-T modified AON **5**. Hence, it is likely that RNA selectivity of each type of cLNA decreases in the following rank: cLNA-G (ΔT_m = 2.9 °C/modification) > cLNA-T (ΔT_m = 2.2 °C/modification) > cLNA-C (ΔT_m = 1.8 °C/modification) > cLNA-A (ΔT_m = 0.9 °C/modification). For AONs **6**−**8**, which contain both cLNA-A and cLNA-G, each cLNA-A and cLNA-G modification seems to lead to a magnitude of RNA selectivity very similar to that found for AON **2** and AON **3**.

3.0. Nuclease Stability Studies of cLNA Modified AONs. Chemically modified AONs are required especially to have

dx.doi.org/10.1021/jo200073q |*J. Org. Chem.* 2011, 76, 4408–4431

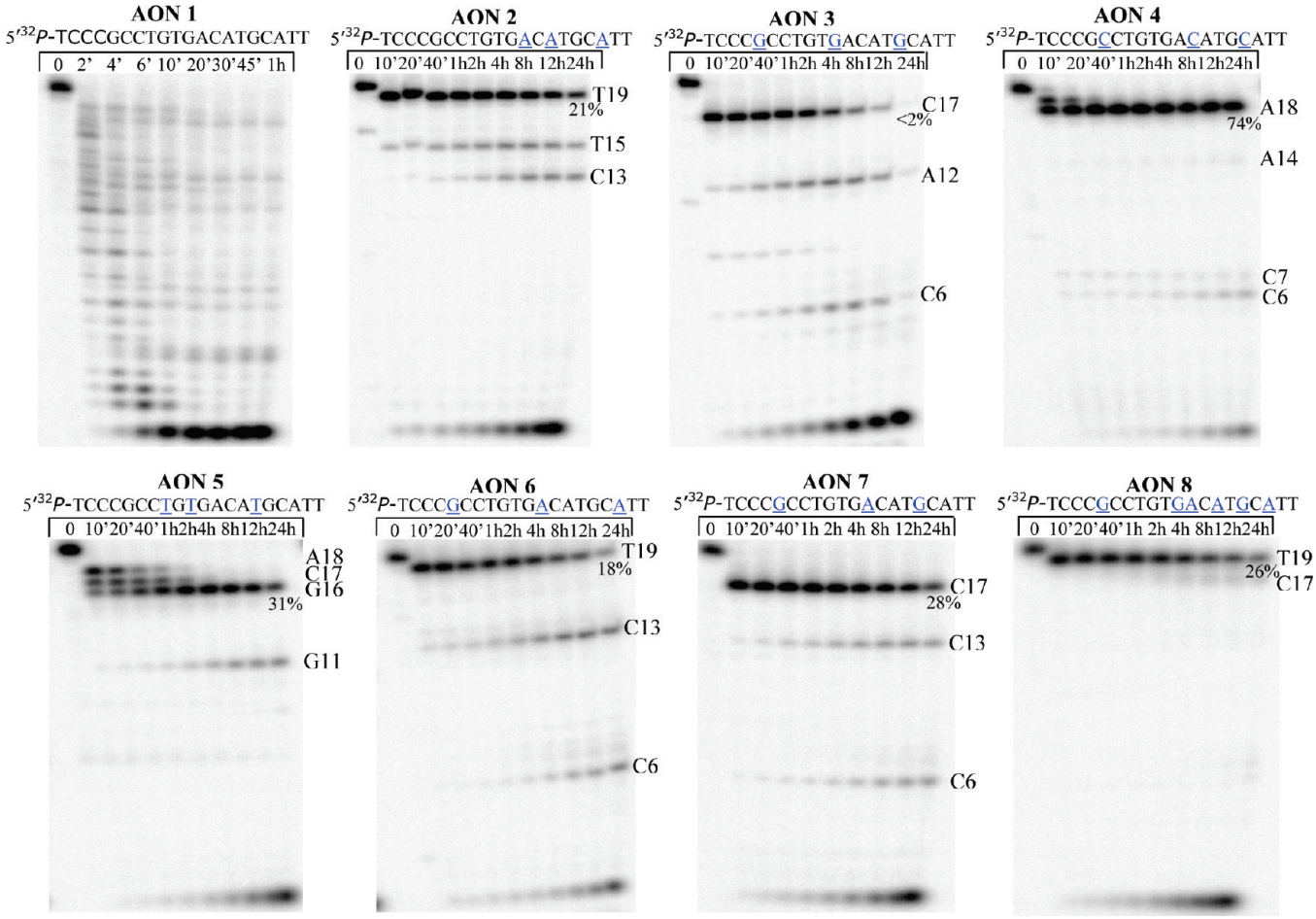

Figure 9. Denaturing PAGE analysis of the SVPDE degradation of AONs with cLNA modifications. The AON % left after 24 h incubation for each AON is shown below the corresponding band. Digestion conditions: AON 3 μM (5′-end ^{32}P labeled with specific activity 80 000 cpm) in 100 mM Tris-HCl (pH 8.0) and 15 mM $MgCl_2$, 21 °C, total reaction volume 30 μL, SVPDE concentration (6.7 ng/μL).

resistance toward nuclease degradation for their in vivo applications, whereas the predominant nuclease activity in vivo comes from 3′-exonuclease.[28] Therefore, the newly synthesized AONs **2**−**8** were treated with 3′-exonuclease (phosphodiesterase I from *Crotalus adamanteus* venom [SVPDE] used in this study) for testing their nuclease stability. The selected AONs were labeled at the 5′-end with ^{32}P and then incubated with SVPDE [SVPDE 6.7 ng/μM, 100 mM Tris-HCl (pH 8.0), 15 mM $MgCl_2$, total volume 30 μL] at 21 °C. Aliquots were taken out at appropriate time intervals and analyzed by 20% denaturing PAGE.

From the gel pictures (Figure 9), we found the native AON **1** was completely degraded in several minutes under the present conditions, while the other cLNA modified AONs **2**−**8** showed considerably improved 3′-exonuclease resistance to a variable extent (most of them stand until 24 h). Because the first modification site from the 3′-end of AON **2**−**8** is located at different positions within the oligo (see Table 1), the band corresponding to 19mer of AON **2**, 17mer of AON **3**, 18mer and 19mer of AON **4**, 16mer plus 17 and 18mer of AON **5**, 19mer of AON **6**, 17mer of AON **7**, and 19mer of AON **8** could be observed on the PAGE pictures (Figure 9).

Since SVPDE has no phosphatase activity, the 5′-^{32}P labels should be intact during SVPDE incubation. Hence, the relative band intensities quantified after autoradiography can reflect their real relative quantity for bands in the same lane. Thus, total percentages of integrated various bands of AONs mentioned above were plotted against time points to give the SVPDE digestion curve for AONs **1**−**8** in Figure 10, and pseudofirst-order reaction rates were obtained by fitting the curves to single-exponential decay functions. A comparison of digestion rates of AON **2**−**8** gave the following results and implications.

3.1. Relative 3′-Exonucleolytic Stabilities of cLNA-A, -G, -^{Me}C, and -T Modified AONs. Through comparison of pseudofirst-order reaction rates, we found that the stabilities of AONs **2**−**8** toward SVPDE incubation decreased in the following order: cLNA-^{Me}C modified AON **4** (k = 0.0002 min^{-1}) > cLNA-T modified AON **5** (k = 0.0008 min^{-1}) > cLNA-G and A modified AON **7** (k = 0.0009 ± 0.0001 min^{-1}) > cLNA-G and A modified AON **6** (k = 0.0013 ± 0.0001 min^{-1}) > cLNA-G and A modified AON **8** (k = 0.0013 ± 0.0001 min^{-1}) > cLNA-A modified AON **2** (k = 0.0014 ± 0.0001 min^{-1}) > cLNA-G modified AON **3** (k = 0.0040 min^{-1}). This result suggests all the cLNA modified AONs **2**−**8** (despite various positions or base modifications) are much more stable than the native counterpart, which degraded completely within several minutes.

3.2. Effect of Various Base Moieties of cLNAs on 3′-Exonucleolytic Stability. We found cLNA-^{Me}C modified AON **4** was the most stable among all cLNA modified AONs. It is 4 times more stable than cLNA-T modified AON **5**, 7 times more stable

dx.doi.org/10.1021/jo200073q |*J. Org. Chem.* 2011, 76, 4408–4431

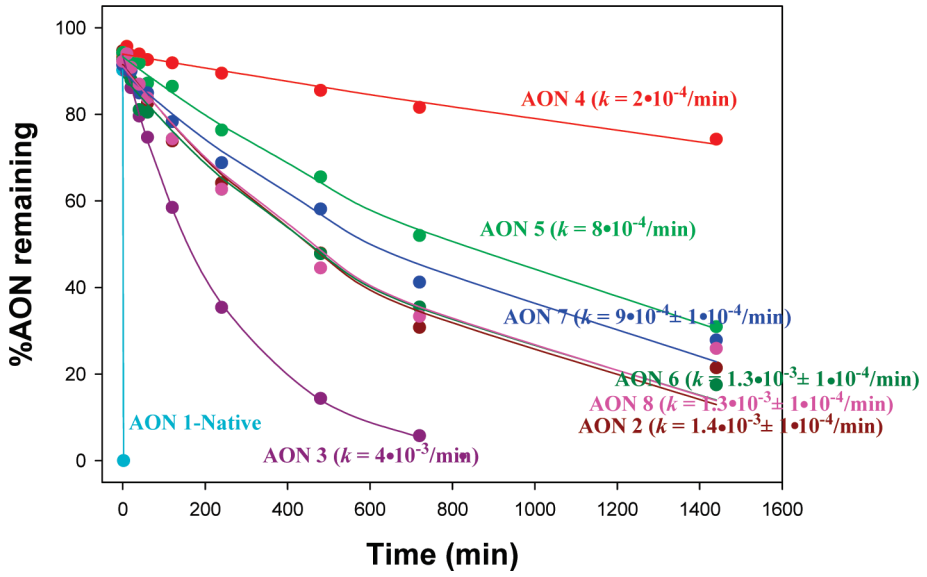

Figure 10. SVPDE digestion curves of native AON **1** and modified AONs **2**−**8**. The pseudofirst-order rates shown here were obtained by fitting the curve to the single-exponential decay function. Digestion conditions: AON 3 μM DNA concentration (5′-end ^{32}P labeled with specific activity 80 000 cpm), 100 mM Tris-HCl (pH 8.0), 15 mM $MgCl_2$, [SVPDE] = 6.7 ng/μL, total reaction volume was 30 μL, 21 °C.

Table 2. Comparison of Michaelis−Menten Kinetic Parameters of Cleavage of Oligonucleotides Modified at the 3′-End with Different Native Deoxyribo- and Ribonucleotides by SVPDE[a]

oligo name	sequence	K_M (μM)	k_{cat} (min^{-1})	k_{cat}/K_M (μM$^{-1}\cdot$min^{-1})	relative k_{cat}/K_M
AON **9**	$(T_p)_{13}T_{ps}T_pT$	2.88 ± 0.65	36.55 ± 2.1	11.8 ± 2.5	1
AON **10**	$(T_p)_{13}T_{ps}T_pC$	2.63 ± 0.59	22.76 ± 1.4	14.0 ± 3.6	1.19
AON **11**	$(T_p)_{13}T_{ps}T_pA$	2.63 ± 0.62	26.2 ± 1.0	11.4 ± 2.0	0.97
AON **12**	$(T_p)_{13}T_{ps}T_pG$	0.66 ± 0.19	13.1 ± 0.7	15.8 ± 7.9	1.34
AON **13**	$(T_p)_{13}T_{ps}T_prU$	1.80 ± 0.32	16.3 ± 0.7	8.3 ± 1.2	0.70
AON **14**	$(T_p)_{13}T_{ps}T_prC$	3.19 ± 0.53	18.58 ± 0.76	5.4 ± 1.5	0.46
AON **15**	$(T_p)_{13}T_{ps}T_prA$	3.97 ± 0.91	19.4 ± 1.1	6.0 ± 3.7	0.51
AON **16**	$(T_p)_{13}T_{ps}T_prG$	3.47 ± 0.81	17.7 ± 1.1	5.6 ± 1.9	0.47

[a] The digestion curves are shown in Supporting Information Figure SI.2−9.

than cLNA-A modified AON **2**, and even 20 times more stable than cLNA-G modified AON **3**. Although given that cLNA-T contains 7′-*R*/*S*-Me product and cLNA-^{Me}C contains 7′-*R*/*S*-Me (**46a**/**b**) and *endo*-product (**46c**) as mixtures, the results of their incorporation into oligonucleotides clearly show their usefulness as RNA-directed agents.[31] Especially for cLNA-^{Me}C, only a small amount (≈10%) of 7′-*S*-Me-cLNA-^{Me}C and the endoproduct (**46c**) exist (≈3−5%) in the mixtures, which is not expected to significantly influence the results of nuclease stability compared to the obvious difference of nuclease resistance between cLNA-^{Me}C and cLNA-T/A/G (see Figure 10). Similarly, the T_m difference found is well within the error limit, given the poor accuracy of the T_m measurement (±0.5 °C among three consecutive measurements). It is noteworthy that while the biochemical properties of oligos containing cLNA-^{Me}C and -T represent the total property contributed by each isomeric component, the properties of cLNA-A/G modified oligos represent the properties contributed by 7′-*R*-Me-cLNA-A and -G. In addition, cLNA-T modified AON **5** (k = 0.0008 min^{-1}) was also found to be more stable than cLNA-A modified AON **2** (k = 0.0014 ± 0.0001 min^{-1}) and cLNA-G modified AON **3** (k = 0.0040 min^{-1}). These results suggest the cLNAs with pyrimidine moieties seemed to give higher nuclease resistance than those of cLNAs with the purine moieties.

3.3. Effect of Various Nucleobase Moieties on 3′-Exonucleolytic Stability for Natural Nucleotides. To figure out if the digestion rate of natural nucleotides by SVPDE is also nucleobase dependent, Michaelis−Menten kinetics analysis of AONs **9**−**16** has been performed. AONs **9**−**16** are 15mer oligonucleotides (with general formula [5′-$(T_p)_{13}T_{ps}T_p$N-3′, where N = A/G/T/C/rA/rG/rU/rC], see Table 2), and the only difference between them is that they have different 3′-end nucleotides (N). For all of them, the second internucleotidyl phosphate linkage from the 3′-end has been modified to phosphorothioate (ps), which is known to be fairly resistant toward SVPDE.[29] Hence, the enzyme only recognizes and cleaves the first nucleotide from the 3′-end at the initial stage of the reaction (see Supporting Information Figure SI.1).

The Michaelis−Menten kinetic parameters for digestion of each oligonucleotide by SVPDE are listed in Table 2. For AONs **9**−**12** which have *deoxyribo*nucleotides (N) in the 3′-end, their digestion efficiencies (k_{cat}/K_M) are in the same magnitude,

dx.doi.org/10.1021/jo200073q |*J. Org. Chem.* 2011, 76, 4408–4431

around 10^1 $\mu M^{-1}\cdot Min^{-1}$. $(T_p)_{13}T_{ps}T_pC$ (AON **10**) and $(T_p)_{13}T_{ps}T_pG$ (AON **12**) can be cleaved slightly faster than $(T_p)_{13}T_{ps}T_pT$ (AON **9**) and $(T_p)_{13}T_{ps}T_pA$ (AON **11**). However, SVPDE digestion of 3′-end *ribo*nucleotides in AONs **13**−**16** was found much slower than digestion of 3′-*deoxy*ribonucleotides in AONs **9**−**12**, which is consistent with a previous report that *deoxyribo*nucleotides are hydrolyzed faster than the *ribo*nucleotides by SVPDE.[30] It seems that both increased K_M and decreased k_{cat} contribute to the decreased digestion efficiency (k_{cat}/K_M) for 3′-*ribo*nucleotides in AONs **13**−**16** compared to digestion of 3′-*deoxyribo*nucleotides in AONs **9**−**12**. The k_{cat}/K_M of digestion of AONs **13**−**16** varied from 5.4 to 8.3 $\mu M^{-1}\cdot min^{-1}$, suggesting SVPDE does not differentiate the different nucleobases among the 3′-end ribonucleotides.

Thus, SVPDE digests of four different native *deoxyribo*nucleotides (AONs **9**−**12**) with similar efficiency (well within the error limit of Michaelis−Menten kinetic parameters) as those found for four different native *ribo*nucleotides (AONs **13**−**16**) show that there is no native nucleobase preference for digestion by SVPDE (Table 2). *Hence, the much different reactivity of cLNA-T, -A, -G, and -*^{Me}*C toward SVPDE, vis-à-vis native counterparts, as described in* Section 3.2, *is a property of cLNAs.*

4.0. Human Blood Serum Studies of Carba-LNAs Modified AONs. The newly synthesized AONs **2**−**8** with modifications of cLNA-A, -G, -^{Me}C, and -T at different positions were also assayed for stability in human blood serum. Thus, the AONs (5′-end ^{32}P labeled) were incubated with human blood serum (male, type AB) for up to 48 h at 21 °C, and aliquots were taken out at regular time intervals and then analyzed by 20% denaturing PAGE. The gel pictures obtained by autoradiography are shown in the Supporting Information Figure SI.10. Because of the presence of alkaline phosphatase in blood serum which gradually removes the 5′-end ^{32}P label, the determination of the accurate degradation rate for each AON by quantifying the gel picture is not possible. Therefore, through visual comparison of the gel pictures, we found nearly all modified 20mer AONs **2**−**8** can sustain in blood serum for more than 48 h, while the native AON **1** can only stand until 12 h under identical conditions. Among all the studied AONs **1**−**8**, cLNA-^{Me}C modified AON **4** was found to be the most stable oligonucleotide upon blood serum treatment, which was well in agreement with that observed upon treatment of 3′-exonuclease. The relative stabilities in blood serum for all modified AONs in the present study are as follows: cLNA-^{Me}C modified AON **4** > cLNA-T modified AON **5** ≈ cLNA-G and A modified AON **8** > cLNA-G modified AON **3** ≈ cLNA-G and A modified AON **6** ≈ cLNA-G and A modified AON **7** > cLNA-A modified AON **2** > native AON **1**. It therefore appeared that the order of relative stabilities of AONs in human blood serum was similar with those observed upon treatment of 3′-exonuclease SVPDE.

5.0. RNase H Digestion Study of cLNA Modified AONs. The RNase H recruitment study of cLNA-A, -G, -^{Me}C, and -T modified AONs **2**−**8** have been carried out and compared with the native AON **1**. From the gel picture (Figure 11), we found for the native AON **1**/RNA hydrid that the *Escherichia coli* RNase H1 cleaves the central part of the RNA strand (between A6 and G14) with a preference on A13. Incorporation of cLNA modifications in the AON strands leads to a stretch of a 5−6 base pairs region in the RNA strand which is completely resistant to RNase H1 mediated cleavage (Figure 12). This is due to the reason that cLNA-T, cLNA-A, G, and ^{Me}C modifications in AON can modulate the conformation 5−6 base pairs region next to the modification site in the 2′-deoxyoligo-AON strand to adopt an RNA-type conformation, which has been evidenced by the change in RNase H cleavage pattern of the corresponding AON:RNA hybrid compared to the native counterpart.[14a−f] By appropriately choosing the cLNA modification sites in the 2′-deoxy-AON strand, the digestion centers of 2′-deoxy-AON:RNA by RNase H can be totally repressed in certain regions or can be engineered to cleave at a specific site (as in catalytic RNA) due to conformational transformation of those site(s) to the RNA:RNA type due to cLNA modifications.

If the modification sites are chosen appropriately as in AON **2**, AON **4**, AON **6**, and AON **7**, the complementary RNA strand of the modified AON:RNA hybrids can be recognized and cleaved by RNase H reflecting the site-specific presence of cLNA modifications. On the contrary, RNase H degradation of the RNA strand in the AON **3**/RNA, AON **5**/RNA, and AON **8**/RNA is totally repressed because in them the modification stretch covers the whole possible cleavage sites (Figure 12).

Hence, we can effectively protect a complementary RNA from RNase H digestion (e.g., for steric blocking using the antisense approach) by engineering an appropriately modified 2′-deoxy-AON in the 2′-deoxy-AON/RNA heteroduplex, as duplexes AON **3**/RNA, AON **5**/RNA, and AON **8**/RNA (Figure 11).

Alternatively, we can, at will, engineer multiple RNA cleavage site or a single RNA cleavage site at a specific point within the RNA strand in the 2′-deoxy-AON/RNA heteroduplex by judiciously choosing the position of cLNA modification in the complementary AON strand, which is evidenced by the single site cleavage at the 3′→ 5′ phosphodiester bond of A13−G14 in the AON **4**/RNA heteroduplex (Figure 11).[31] This cLNA modified oligonucleotide-induced engineering of a specific cleavage point in the complementary RNA strand with the help of RNase H (which is omnipresent in the mammalian cells) is reminiscent of the characteristic RNA cleavage at a single cleavage site found in RNA catalysis because of the change brought about by the change of the internal folding motif within RNA with or without a cofactor as in, e.g., hairpin ribozyme, or those induced by a second RNA strand (e.g., hammerhead) or in DNAzyme in which the RNA folding motif is induced by a complexing DNA strand.

Additionally, certain specific cLNA modification in AON, as in the AON **4**/RNA heteroduplex, made the corresponding 2′-deoxy-AON:RNA hybrid an almost 2-fold better substrate to RNase H (Figure 13). So what we show here is that simple designer construction of cLNA modified 2′-deoxyoligo, when complexed to complementary RNA, can in fact perform a dual job with the help of RNase H ((a) specific cleavage of the complementary RNA strand at a specific site) and can also cause a (b) considerable enhancement of the RNA cleavage rate compared to that of the native.

So, we present evidence that shows that these cLNA modified oligos can become an important tool for RNA engineering which potentially can complement ribozyme function.

For AON **1**/RNA, AON **2**/RNA, AON **4**/RNA, AON **6**/RNA, and AON **7**/RNA, total percentages of intact RNA were plotted against time points to give the RNase H digestion curve for every AON:RNA hybrid, and pseudofirst-order reaction rates were obtained by fitting the curves to single-exponential decay functions. Through comparison of digestion rates of each AON:RNA hybrid (Figure 13), we have found that the cleavage rates of AON **2**, **6**, or **7**/RNA hybrids are only around half that of the native AON:RNA hybrid, while the cLNA-^{Me}C modified AON

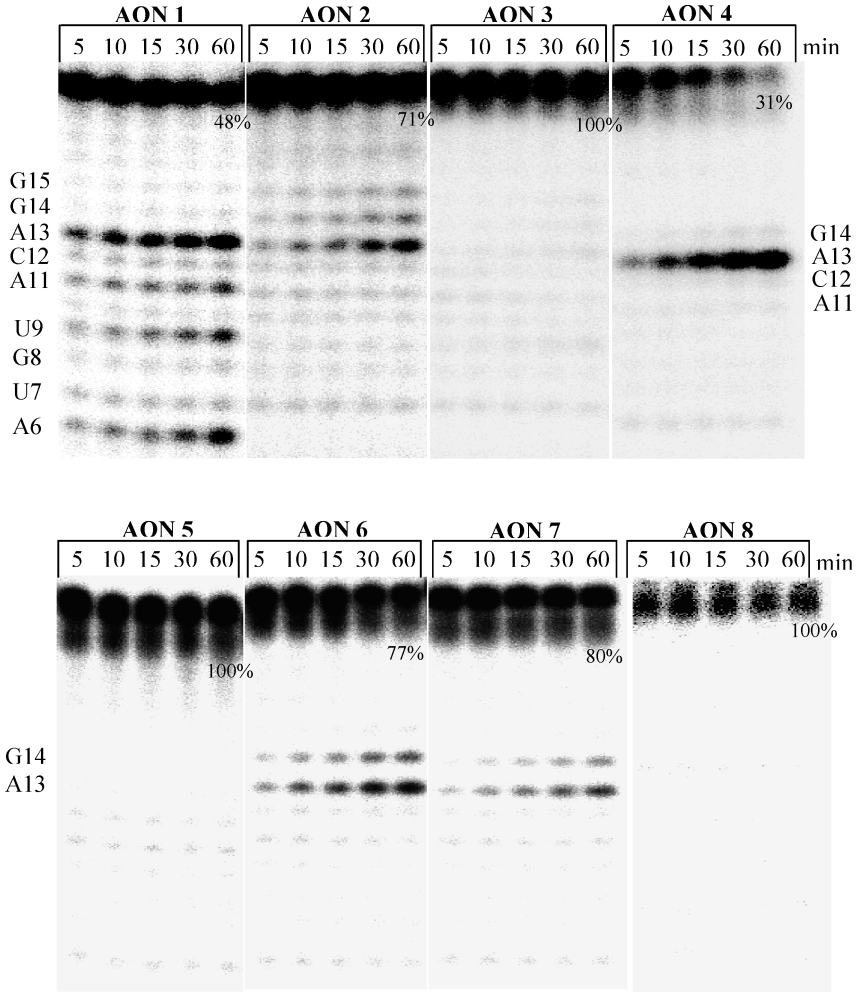

Figure 11. Autoradiograms of 20% denaturing PAGE pictures, showing the cleavage kinetics of 5′-^{32}P-labeled target RNA by *E. coli* RNase H1 in the AON/RNA hybrids. The intact RNA% left after 1 h incubation for each AON/RNA is shown below the corresponding band. Conditions of cleavage reactions: RNA (0.1 μM) and AONs (2 μM) in buffer containing 20 mM Tris-HCl (pH 8.0), 20 mM KCl, 10 mM $MgCl_2$, and 0.1 mM DTT at 21 °C, 0.08 U of RNase H1, total volume 30 μL.

4/RNA hybrid exhibits 2 times higher cleavage rate compared to the native AON:RNA hybrid. Given the fact that AON **2**/RNA, AON **4**/RNA, AON **6**/RNA, and AON **7**/RNA showed a very similar cleavage pattern by RNase H (Figures 11 and 12) but with much different cleavage rates (Figure 13), we can arrive at the conclusion that cLNA-A, -G, -T, and -^{Me}C nucleoside modification in the same AON sequence can lead to a much different effect on RNase H digestion efficiency.

■ CONCLUSIONS AND IMPLICATIONS

In the present study, cLNA-A, -G, and cLNA-^{Me}C nucleosides have been synthesized through an intramolecular radical cyclization. Biological properties of AONs containing 7′*R*-Me-cLNA-A, 7′*R*-Me-cLNA-G, and (*exo*/*endo* products) cLNA-^{Me}C modifications have been evaluated and compared with 7′*R*/*S*-Me-cLNA-T[14a] modified counterpart as well as with that of the native AON. The major conclusions are as follows:

(1) All the cLNAs-A, -G, and -^{Me}C modified 20mer AONs showed improved RNA affinity compared to the native counterpart, but pyrimidine-type cLNA-^{Me}C (+2.5 °C/modification) and cLNA-T (+3 °C/modification) modifications showed higher RNA affinity than purine type cLNA-G (+2 °C/modification) and cLNA-A (+1 °C/modification) modifications. For an explanatory note of why AON/RNA duplexes are generally more stable than the AON/DNA counterpart, see ref 32.

(2) All the cLNAs-A, G, and ^{Me}C modified 20mer AONs were found to be RNA selective. One cLNAs-G modification (ΔT_m = 2.9 °C/modification) leads to the greatest RNA selectivity, and one cLNA-A modification leads to the least RNA selectivity (ΔT_m = 0.9 °C/modification), with cLNA-T (ΔT_m = 2.2 °C/modification) and cLNA-^{Me}C (ΔT_m = 1.8 °C/modification) in between.

(3) The nucleolytic stability of cLNA was found to vary greatly with different nucleobase moieties. cLNA-^{Me}C modified AON was found to be most stable toward SVPDE, followed by cLNA-T and cLNA-A modified counterparts. cLNA-G modified AON was found to be most labile. On the contrary, studies using native DNA and RNA models showed that SVPDE exhibited very similar activity toward four deoxyribonucleotides as well

dx.doi.org/10.1021/jo200073q |*J. Org. Chem.* 2011, 76, 4408–4431

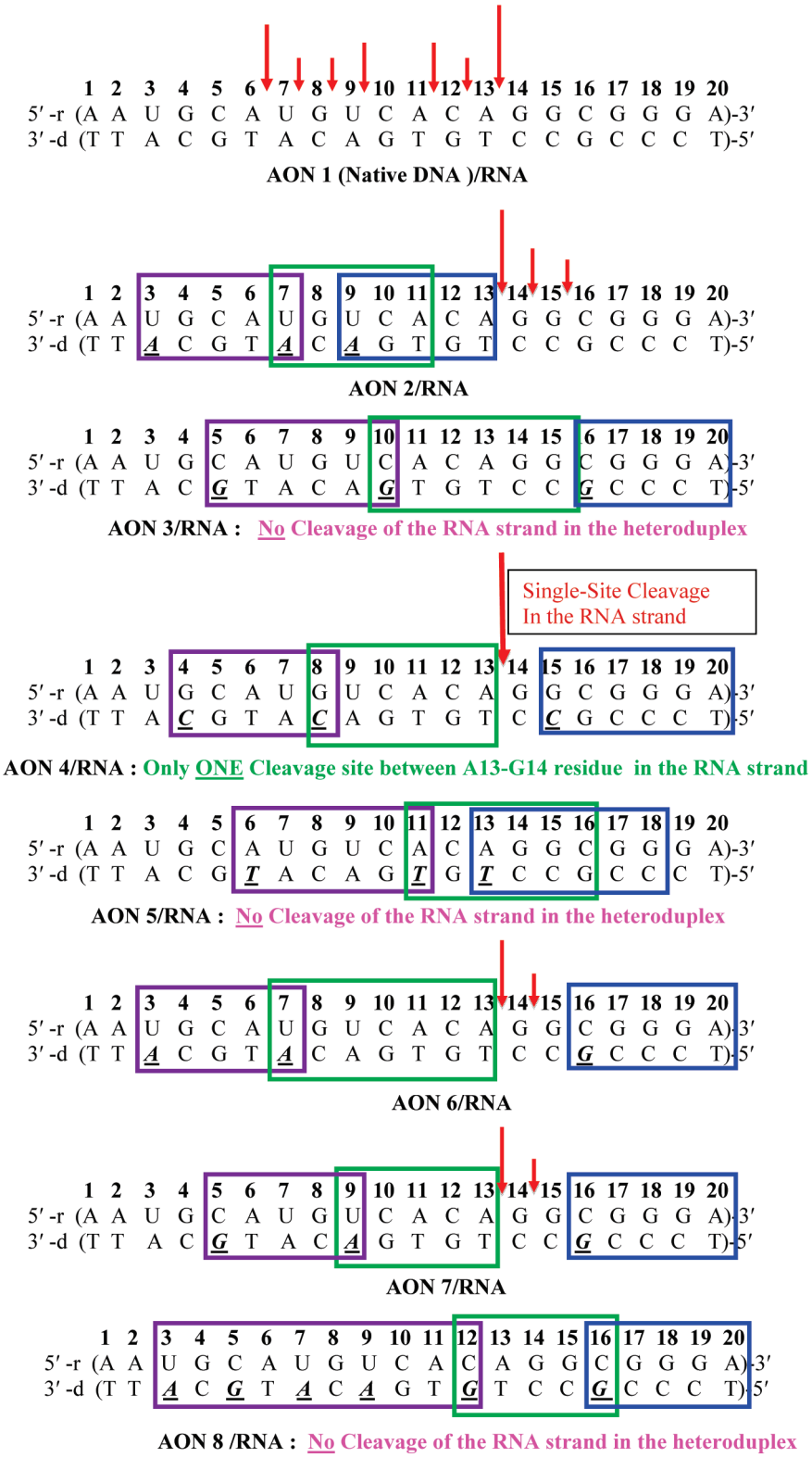

Figure 12. RNase H1 cleavage pattern of hybrid duplexes. Modifications in the 2′-deoxy-AON strand in the heteroduplex are shown by an underscore + italic + bold. The boxes show the conformational transmission effect to RNA-type conformation in the AON strand owing to North-locked cLNA modification(s) in the proximity, and hence the resulting RNA:RNA pseudoduplex is uncleavable by RNase as evidenced by PAGE footprints in Figure 11. The vertical "red" arrows show the RNA cleavage sites, and the relative length of an arrow shows the relative extent of cleavage at that site. The square boxes show the stretch of the modification, which is resistant to RNase H1 cleavage. Duplexes AON **3**/RNA, AON **5**/RNA, and AON **8**/RNA can not be degraded by RNase H because of their overlapping resistance region owing to cLNA modification stretch over the whole possible cleavage sites. On the other hand, heteroduplex AON **4**/RNA has been designed such that we have engineered a single cleavage site in the target RNA strand.

dx.doi.org/10.1021/jo200073q |*J. Org. Chem.* 2011, 76, 4408–4431

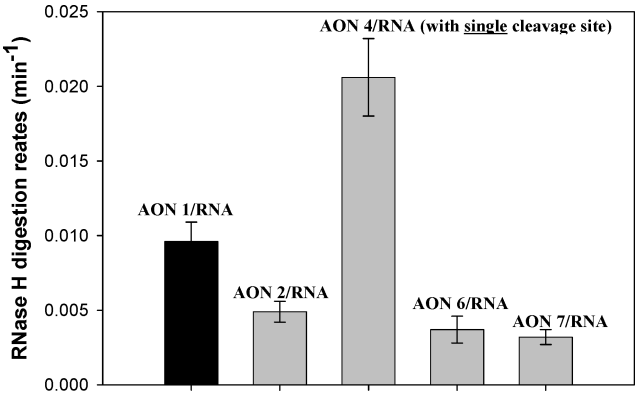

Figure 13. Bar plots show the cleavage rates of RNase H1 mediated degradation of RNA in native and modified AON:RNA hybrid duplexes. Duplexes AON **3**/RNA, AON **5**/RNA, and AON **8**/RNA can not be degraded by RNase H, and hence they are not shown here. On the other hand, the cleavage rate of the AON **4**/RNA heteroduplex (with a single cleavage site) is ca. 2-fold better than that of the native AON **1**/RNA counterpart.

as four ribonucleotides. Hence, the discrimination of various cLNA modified nucleotides in AON by SVPDE is a unique property of the cLNAs.

(4) Just like cLNA-T, cLNA-A, G, and ^{Me}C, modifications in AON change the RNase H cleavage pattern for the AON/RNA hybrid. By appropriately choosing the modification sites in AON strands, the digestion of AON/RNA can be totally repressed or limited to cleavage at a specific site.

(5) When the cleavage patterns are the same, cLNA-^{Me}C modified AON/RNA can be degraded by RNase H nearly four times faster than cLNA-A and c-LNA-G modified counterparts and two times faster than the native counterpart.

(6) It has been shown that cLNA-T, cLNA-A, G, and ^{Me}C modifications in AON can modulate the neighboring nucleotides (up to 5−6 nucleotides) to adopt an RNA-type conformation, which has been evidenced by the change in the RNase H cleavage pattern of the corresponding AON/RNA hybrid compared to the native counterpart. By appropriately choosing the cLNA modification sites in the 2′-deoxy-AON strand, the digestion centers of 2′-deoxy-AON/RNA by RNase H can be totally repressed in certain regions or can be engineered to cleave at a specific site (as in catalytic RNA). Additionally, certain specific cLNA modification in AON made the corresponding 2′-deoxy-AON/RNA hybrid almost a 2-fold better substrate to RNase H than that of the native. So what we show here is that simple designer construction of the cLNA modified oligo, when complexed to complementary RNA, can in fact perform a dual job with the help of RNase H: (a) it can cause specific cleavage of complementary RNA at a specific site, and (b) it also can promote a considerable enhancement of the cleavage rate compared to that of the native.

(7) Recently, carba-LNA (cLNA) incorporated antisense oligonucleotides (AON) and siRNA have been studied against various biological targets to evaluate the true potential of cLNA in various disease models like the single cell replication model for HIV-1 [*Med. Chem. Commun.* **2011**, *2*, 206] and allele selective inhibition of Mutant *Huntingtin* expression [*Biochemistry* **2010**, *49*, 10166−10178] involving cell culture in vitro and in vivo experiments. These studies clearly showed that cLNA is better than any other modification including LNA in term of IC_{50}, selective inhibition of HTT, and human blood serum stability. Apart from these studies, Seth et al. [*J. Am. Chem. Soc.* **2010**, *132*, 14942−14950] also have studied the potential of cLNA versus LNA and methylene-cLNA in cell culture (brain endothelial cells using electroporation) and animal experiments (subchronic dosing schedule in mice). They found that cLNA was slightly less potent compared to LNA and methylene-cLNA modified AONs under employed experimental conditions. It is also clear that it is not always straightforward to understand why particularly modified AONs are more effective than others, especially with such a wide variety of targets and experimental conditions. A number of factors can complicate an oligonucleotide's ability to reach its target RNA and inhibit gene expression. Simple explanations might include poor transfection or release from endosomes after cell entry and cellular uptake (see footnote under ref 33 for exact AONs or siRNA construct).

(8) We also present experimental evidence that shows that these cLNA modified oligos can become an important tool for RNA engineering which potentially can complement a ribozyme action.

(9) Taken together, cLNA-^{Me}C modified antisense oligonucleotides exhibit higher RNA affinity, RNA selectivity, greatly improved nuclease stability, and efficient RNase H recruitment capability compared to cLNA-A, -G, and -T modified counterparts. Hence, in a mixed sequence the modification with cLNA-^{Me}C nucleotide units could be more preferentially recommended than other cLNAs in a promising therapeutic antisense or siRNA for RNA targeting and inhibition.

■ EXPERIMENTAL SECTION

9-[4-*C*-Allyl-3,5-di-*O*-benzyl-2-*O*-acetyl-*β*-D-ribofuranosyl]-N^6-benzoyladenine (38a). Compound **36** (25.0 g, 60.93 mmol) was dissolved with acetic anhydride (65 mL, 686 mmol) and acetic acid (347 mL) and cooled to 0 °C, and then triflic acid (0.5 mL) was added to this mixture. After 30 min of stirring at 0 °C, the reaction was quenched with cold saturated $NaHCO_3$ solution and extracted with DCM. The organic layer was dried and evaporated. The obtained residue was coevaporated with dry CH_3CN (3 × 650 mL) and dissolved in the same (650 mL). N^6-Benzoyladenine (16 g, 66 mmol) and *N*, *O*-bis(trimethylsilyl)acetamide (33.3 mL, 144 mmol) were added to this solution and refluxed for 45 min. The solution was cooled to 0 °C, and TMSOTf (15 mL, 82 mmol) was added dropwise and then allowed to warm to 50 °C and kept constant at this temperature overnight. The reaction was quenched with saturated NH_4Cl solution and was extracted with EtOAc (3 × 450 mL). The organic layer was dried and evaporated, and the obtained residue was subjected to column chromatography over silica gel eluting with 70% EtOAc in hexane (v/v) to give **38a** as a white foam (30 g, 86%): R_f 0.60 (5% methanol in DCM, v/v). ^{1}H NMR (600 MHz, $CDCl_3$): δ 8.98 (1H, s, NH), 8.77 (1H, s, H2), 8.33 (1H, s, H8), 8.02 (2H, d, J = 7.8 Hz, Ar−H), 7.60 (1H, t, J = 7.8 Hz, Ar−H), 7.52 (2H, t, J = 7.8 Hz, Ar−H), 7.2−7.4 (10H, m, Ar−H), 6.40 (1H, d, J = 4.8 Hz, H1′), 5.92 (1H, t, J = 4.8 Hz, H2′), 5.8−5.95 (1H, m, H7′), 5.10 (1H, d,

dx.doi.org/10.1021/jo200073q |*J. Org. Chem.* 2011, 76, 4408–4431

J = 4.8 Hz, H8′), 5.08 (1H, m, H8′), 4.63 (1H, d, J = 11.4 Hz, CH_2Ph), 4.58 (1H, d, J = 5.4 Hz, H3′), 4.53 (2H, t, J = 10.8 Hz, CH_2Ph), 4.44 (1H, d, J = 12 Hz, CH_2Ph), 3.64 (1H, d, J = 10.2 Hz, H5″), 3.42 (1H, d, J = 10.2 Hz, H5′), 2.72 (1H, dd, J = 6 and 15 Hz H6″), 2.41 (1H, dd, J = 8.4 and 14.4 Hz, H6′), 2.07 (3H, s, CH_3). ^{13}C NMR (150.9 MHz, $CDCl_3$): δ 169.9 (CH_3C═O), 164.5 (PhC═O), 152.7 (C2), 151.8 (C4), 149.4 (C6), 141.8 (C8), 137.5 (Ar−C), 137.4 (Ar−C), 137.2 (Ar−C), 133.8 (Ar−C), 132.7 (C7′), 129.9 (Ar−C), 128.9 (Ar−C), 128.7 (Ar−C), 128.6 (Ar−C), 128.53 (Ar−C), 128.49 (Ar−C), 128.1 (Ar−C), 128 (Ar−C), 127.9 (Ar−C), 127.8 (Ar−C), 127.7 (Ar−C), 123.2 (C5), 118.6 (C8′), 87.9 (C4′), 85.9 (C1′), 78.3 (C3′), 75.7 (C2′), 74.4 (CH_2Ph), 73.6 (CH_2Ph), 72.5 (C5′), 37.2 (C6′), 20.6 (CH_3). MALDI-TOF m/z $[M+H]^+$ calcd for $C_{36}H_{36}N_5O_6$ 634.267, found 634.264.

9-[4-*C*-Allyl-3,5-di-*O*-benzyl-β-D-ribofuranosyl]-N^6-benzoyladenine (39a). Compound **38a** (30 g, 47.4 mmol) was dissolved in THF (120 mL) and cooled to 0 °C, to which a cold solution of NaOH (7.5 g, 189 mmol) in water (90 mL) was added dropwise over 15 min at the same temperature, and the mixture was allowed to warm to rt and stirred for another 2 h. The reaction mixture was quenched with water and extracted with EtOAc (300 mL). The organic layer was dried over Na_2SO_4, concentrated under reduced pressure, and dried under vacuum to give crude **39a** as an off-white foam (27.0 g, 97%). ^{1}H NMR (600 MHz, $CDCl_3$): δ 9.14 (1H, s, NH), 8.70 (1H, s, H2), 8.19 (1H, s, H8), 7.99 (2H, d, J = 7.8 Hz, Ar−H), 7.58 (1H, t, J = 7.2 Hz, Ar−H), 7.49 (2H, t, J = 7.2 Hz, Ar−H), 7.2−7.4 (10H, m, Ar−H), 6.10 (1H, d, J = 5.4 Hz, H1′), 5.82−5.91 (1H, m, H7′), 5.08−5.16 (2H, m, H8′ and H8″), 4.89 (1H, m, J = 4.8 Hz, H2′), 4.76 (1H, d, J = 11.4 Hz, CH_2Ph), 4.72 (1H, d, J = 11.4 Hz, CH_2Ph), 4.53 (1H, d, J = 12 Hz, CH_2Ph), 4.47 (1H, d, J = 11.4 Hz, CH_2Ph), 4.38 (1H, d, J = 5.4 Hz, H3′), 3.78 (1H, d, J = 4.8 Hz, O*H*), 3.59 (1H, d, J = 10.2 Hz, H5″), 3.46 (1H, d, J = 9.6 Hz, H5′), 2.77 (1H, dd, J = 6 and 14.4 Hz, H6″), 2.46 (1H, dd, J = 8.4 and 14.4 Hz, H6′). ^{13}C NMR (150.9 MHz, $CDCl_3$): δ 164.5 (PhC═O), 152.5 (C2), 151.6 (C4), 149.4 (C6), 141.8 (C8), 137.4 (Ar−C), 137.1 (Ar−C), 133.76 (Ar−C), 132.86 (C7′), 132.7 (Ar−C), 128.8 (Ar−C), 128.7 (Ar−C), 128.6 (Ar−C), 128.5 (Ar−C), 128.3 (Ar−C), 128.1 (Ar−C), 128.0 (Ar−C), 127.8 (Ar−C), 127.7 (Ar−C), 123.1 (C5), 118.6 (C8′), 89.0 (C1′), 87.8 (C4′), 80.2 (C3′), 75.5 (C2′), 74.8 (CH_2Ph), 73.7 (CH_2Ph), 73.1 (C5′), 37.2 (C6′). MALDI-TOF m/z $[M + H]^+$ calcd for $C_{34}H_{34}N_5O_5$ 592.256, found 592.253.

9-[4-*C*-Allyl-3,5-di-*O*-benzyl-2-*O*-phenoxythiocarbonyl-β-D-ribofuranosyl]-N^6-benzoyladenine (40a). Compound **39a** (27.0 g, 45.76 mmol) was dissolved in 400 mL of dry DCM and was cooled to 0 °C. To this precooled solution was added 1-methyl imidazole (14.4 mL, 183 mmol), and the solution was stirred for 20 min at the same temperature. This was followed by addition of phenyl chlorothionoformate (19 mL, 137 mmol) dropwise, and the reaction was stirred for 5 h at room temperature. The reaction was quenched with saturated $NaHCO_3$ solution and extracted with DCM (3 × 350 mL). The organic layer was washed with saturated citric acid solution several times and dried over Na_2SO_4 and concentrated, and the crude compound was chromatographed over silica gel (1% methanol in DCM, v/v) to give **40a** as off-white foam solid (30 g, 90%). R_f 0.60 (3% methanol in DCM, v/v). ^{1}H NMR (500 MHz, $CDCl_3$): δ 9.0 (1H, bs, N*H*), 8.76 (1H, s, H2), 8.33 (1H, s, H8), 8.01 (2H, d, J = 7.75 Hz, Ar−H), 7.57−7.62 (1H, m, Ar−H), 7.49−7.55 (2H, m, Ar−H), 7.23−7.40 (13H, m, Ar−H), 6.95 (2H, d, J = 8 Hz, Ar−H), 6.58 (1H, d, J = 5.5 Hz, H1′), 6.46 (1H, t, J = 5.5 Hz, H2′), 5.80−5.88 (1H, m, H7′), 5.08−5.16 (2H, m, H8′ and H8″), 4.75−482 (2H, m, H3′and CH_2Ph), 4.63 (1H, d, J = 11. Hz, CH_2Ph), 4.59 (1H, d, J = 11 Hz, CH_2Ph), 4.51 (1H, d, J = 9 Hz, CH_2Ph), 3.68 (1H, d, J = 10 Hz, H5″), 3.50 (1H, d, J = 10 Hz, H5′), 2.74 (1H, dd, J = 6.5 and 14.5 Hz, H6″), 2.46 (1H, dd, J = 8.0 and 14.5 Hz, H6′). ^{13}C NMR (125.8 MHz, $CDCl_3$): δ 194.1 (−CSOPh), 164.6 (PhC═O), 153.3 (Ar−C), 152.7 (C2), 151.9 (C4), 149.4 (C6), 141.8 (C8), 137.34 (Ar−C), 137.2 (Ar−C), 133.6 (Ar−C), 132.7 (Ar−C), 132.5 (C7′), 129.6 (Ar−C), 129.5 (Ar−C), 129.3 (Ar−C), 128.8 (Ar−C), 128.7 (Ar−C), 128.6 (Ar−C), 128.5 (Ar−C), 128.2 (Ar−C), 128.14 (Ar−C), 128.09 (Ar−C), 128 (Ar−C), 127.9 (Ar−C), 127.8 (Ar−C), 127.7 (Ar−C), 126.8 (Ar−C), 123.1 (C5), 121.6 (Ar−C), 118.8 (C8′), 88.2 (C4′), 85.0 (C1′), 83.6 (C2′), 78.2 (C3′), 74.8 (CH_2Ph), 73.7 (CH_2Ph), 73.0 (C5′), 37.3 (C6′). MALDI-TOF m/z $[M + H]^+$ calcd for $C_{41}H_{38}N_5O_6S$ 728.254, found 728.249.

(1*R*,3*R*,4*R*,5*R*,7*S*)-3-(N^6-Benzoyladenin-9-yl)-7-benzyloxy-1-benzyloxymethyl-5-methyl-2-oxa-bicyclo[2.2.1]heptane (41a), (1*R*,3*R*,4*R*,5*S*,7*S*)-3-(N^6-Benzoyladenin-9-yl)-7-benzyloxy-1-benzyloxymethyl-5-methyl-2-oxa-bicyclo[2.2.1]heptane (41b), and (1*R*,5*R*,7*R*,8*S*)-7-(N^6-Benzoyladenin-9-yl)-8-benzyloxy-5-benzyloxmethyl-6-oxa-bicyclo[3.2.1]octane (41c). Compound **40a** (10.0 g, 13.7 mmol) was dissolved in dry toluene (400 mL) and bubbled with N_2 gas for 30 min. Bu_3SnH (3.7 mL, 13.7 mmol) was dissolved in 40 mL of toluene, and half of this solution was added dropwise to refluxing solution over 30 min. AIBN (2.3 g, 13.7 mmol) was dissolved in 40 mL of dry toluene and added to the above solution dropwise, and simultaneously the remaining solution of Bu_3SnH was added over 60−70 min. After 60 min of reflux, the solution was cooled, CCl_4 (10 mL) added, and the mixture stirred for 20 min. A solution of iodine in DCM was added to the above solution until a faint coloration persisted, and then solvent was evaporated. The organic layer was dried, evaporated, and chromatographed over silica gel (10−32% EtOAc in hexane, v/v) to give pure **41a** as an off-white foam (3.0 g, 38%). R_f 0.4 (60% EtOAc in hexane, v/v). The remaining mixture was subjected to preparative HPLC separation to yield compound **41b** as white foam solid (0.30 g, 3.95%) (R_f 0.35, 60% EtOAc in hexane, v/v) and white solid **41c** (0.29 g, 3.89%) (R_f 0.35, 60% EtOAc in hexane, v/v).

41a: ^{1}H NMR (400 MHz, $CDCl_3$): δ 9.06 (1H, s, NH-Bz), 8.77 (1H, s, H2), 8.47 (1H, s, H8), 8.03 (2H, d, J = 7.72 Hz, Ar−H), 7.20−7.60 (1H, m, Ar−H), 7.49−7.51 (2H, m, Ar−H), 7.26−7.35 (8H, m, Ar−H), 7.10−7.20 (2H, m, Ar−H), 6.24 (1H, s, H1′), 4.66 (1H, d, J = 12.48 Hz, CH_2Ph), 4.59 (1H, d, J = 12.36 Hz, CH_2Ph), 4.40 (2H, q, J = 14.4 Hz, CH_2Ph), 4.20 (1H, s, H3′), 3.75 (1H, d, J = 11.0 Hz, H5′), 3.66 (1H, d, J = 11.0 Hz, H5′), 2.77 (1H, d, J = 3.4 Hz, H2′), 2.63−2.76 (1H, m, H7′), 2.10 (1H, dd, J = 8.6 and 19.6 Hz, H6″), 1.35 (3H, d, J = 7.24 Hz, 7′-CH_3), 1.26 (1H, dd, J = 4.76 and 12.72 Hz, H6′). ^{13}C NMR (125.8 MHz, $CDCl_3$): δ 164.6 (PhC═O), 152.4 (C2), 150.7 (C4), 149.2 (C6), 141.8 (C8), 137.9 (Ar−C), 137.5 (Ar−C), 133.7 (Ar−C), 132.7 (Ar−C), 128.8 (Ar−C), 128.5 (Ar−C), 128.3 (Ar−C), 127.9 (Ar−C), 127.88 (Ar−C), 127.8 (Ar−C), 127.7 (Ar−C), 127.6 (Ar−C), 127.4 (Ar−C), 123.8 (C5), 88.8 (C4′), 83.4 (C1′), 80.3 (C3′), 73.5 (CH_2Ph), 72.1 (CH_2Ph), 67.4 (C5′), 48.2 (C2′), 37.7 (C6′), 28.7 (C7′), 15.7(CH_3). MALDI-TOF m/z $[M + H]^+$ calcd for $C_{34}H_{34}N_5O_4$ 576.261, found 576.259. **41b**: ^{1}H NMR (500 MHz, $CDCl_3$): δ 9.23 (1H, s, NH-Bz), 8.79 (1H, s, H2), 8.51 (1H, s, H8), 8.04 (2H, d, J = 7 Hz, Ar−H), 7.58−7.62 (1H, m, Ar−H), 7.50−7.55 (2H, m, Ar−H), 7.13−7.40 (10H, m, Ar−H), 5.89 (1H, s, H1′), 4.69 (1H, d, J = 12.5 Hz, CH_2Ph), 4.61 (1H, d, J = 12.5 Hz, CHPh), 4.47 (1H, d, J = 11.5 Hz, CHPh), 4.40 (1H, d, J = 11.5 Hz, CHPh), 4.12 (1H, s, H3′), 3.78 (2H, q, J = 11.0 Hz, H5′/5″), 2.70 (1H, s, H2′), 2.25−2.33 (1H, m, H7′), 2.06 (1H, dd, J = 9 and 12 Hz, H6″), 1.64 (1H, dd, J = 5.5 and 12.5 Hz, H6′), 1.29 (3H, d, J = 7 Hz, 7′-CH_3). ^{13}C NMR (125.8 MHz, $CDCl_3$): δ 164.9 (C═O), 152.0 (C2), 150.8 (C6), 149.3 (C4), 142.8 (C8), 137.7 (Ar−C), 137.6 (Ar−C), 132.7 (Ar−C), 129.4 (Ar−C), 129.0 (Ar−C), 128.6 (Ar−C), 128.4 (Ar−C), 128.4 (Ar−C), 128.0 (Ar−C), 127.9 (Ar−C), 127.8 (Ar−C), 127.7 (Ar−C), 127.4 (Ar−C), 123.7 (C5), 88.5 (C4′), 88.1 (C1′), 79.8 (C3′), 73.5 (CH_2Ph), 72.3 (CH_2Ph), 67.0 (C5′), 48.1 (C2′), 36.6 (C6′), 33.7 (C7′), 20.2 (7′-CH_3). MALDI-TOF m/z $[M + H]^+$ calcd for $C_{34}H_{34}N_5O_4$ 576.261, found 576.264. **41c**: ^{1}H NMR (500 MHz, $CDCl_3$): δ 9.47 (1H, s, N*H*), 8.85 (1H, s, H8), 8.77 (1H, s, H2), 7.50−8.07 (5H, m, Ar−H), 7.23−7.36 (10H, m, Ar−H), 6.32 (1H, s,

H1′), 4.38−4.68 (4H, m, 2 × CH_2Bn), 4.39 (1H, d, J = 5.0 Hz, H3′), 3.64 (1H, d, J = 10.5 Hz, H5″), 3.52 (1H, d, J = 10.5 Hz, H5′), 2.76 (1H, s, H2′), 2.02 (1H, m, H8″), 1.72−1.90 (4H, m, H6″, H7′, H7″, H8′), 1.40 (1H, dd, H6′). ^{13}C NMR (125.8 MHz, $CDCl_3$): δ 164.9 (C═O), 152.2 (C2), 150.8 (C4), 149.3 (C6), 142.0 (C8), 137.7 (Ar−C), 137.6 (Ar−C), 133.1 (Ar−C), 132.7 (Ar−C), 128.8 (Ar−C), 128.6 (Ar−C), 128.4 (Ar−C), 128.1 (Ar−C), 127.9 (Ar−C), 127.8 (Ar−C), 127.7 (Ar−C), 127.4 (Ar−C), 123.6 (C5), 86.9 (C1′), 85.1 (C4′), 73.7 (C3′), 73.3 (CH_2Ph), 71.9 (CH_2Ph), 70.2 (C5′), 42.9 (C2′), 26.7 (C6′), 21.0 (C8′), 17.8 (C7′). MALDI-TOF m/z $[M + H]^+$ calcd for $C_{34}H_{34}N_5O_4$ 576.261, found 576.263.

(1*R*,3*R*,4*R*,5*R*,7*S*)-3-(Adenin-9-yl)-7-hydroxyl-1-(hydroxymethyl)-5-methyl-2-oxa-bicyclo [2.2.1]heptane (44a). Compound **41a** (9 g, 15.65 mmol) was dissolved in methanolic ammonia (400 mL) and stirred for 16 h at room temperature. The reaction mixture was concentrated under vacuum to give **41a**′ as a crude gummy solid. R_f = 0.19 (100% EtOAc). To a solution of **41a**′ (8 g, 16.9 mmol) in methanol (500 mL) were added 20% $Pd(OH)_2$/C (8 g) and ammonium formate (64.2 g, 1019 mmol), and the solution was heated at 60 °C for 16 h in a water bath. The reaction was allowed to reach to rt, and the suspension was filtered over Celite. $Pd(OH)_2$/C was washed with (5 × 400 mL) methanol. The organic solvent was evaporated, and then the dried residue was washed with EtOAc (150 mL) to give **44a** as white powder (3.2 g, 64%). R_f 0.11 (10% methanol in DCM, v/v). ^{1}H NMR (400 MHz, DMSO-d_6): δ 8.24 (1H, s, H8), 8.10 (1H, s, H2), 7.23 (2H, s, NH_2, D_2O exchangeble), 6.00 (1H, s, H1′), 5.27 (1H, d, J = 3.6 Hz, 3′-O*H*, D_2O exchangeble), 4.93 (1H, t, J = 5.7 Hz, 5′-O*H*, D_2O exchangeble), 4.16 (1H, s, H3′), 3.50−3.70 (2H, m, H5′ and H5″), 2.50−2.73 (1H, m, H7′), 2.38 (1H, d, J = 3.12 Hz, H2′), 1.90 (1H, t, J = 12.2 Hz, H6′), 1.20 (3H, d, J = 7 Hz, CH_3), 0.98 (1H, dd, J = 5 and 12.5 Hz, H6′). ^{13}C NMR (125.8 MHz, $CDCl_3$): δ 155.8 (C6), 152.4 (C2), 148.2 (C4), 138.2 (C8), 119.2 (C5), 89.8 (C4′), 81.8 (C1′), 71.9 (C3′), 58.8 (C5′), 50.1 (C2′), 36.7 (C6′), 28.1 (C7′), 15.5 (CH_3). MALDI-TOF m/z $[M + H]^+$ calcd for $C_{13}H_{18}N_5O_3$ 292.141, found 292.139.

(1*R*,3*R*,4*R*,5*R*,7*S*)-3-(*N*^{6}-Benzoyladenin-9-yl)-7-hydroxyl-1-hydroxymethyl-5-methyl-2-oxa-bicyclo[2.2.1]heptane (45a). Compound **44a** (0.5 g, 1.7 mmol) was coevaporated twice with dry pyridine (15 mL) and suspended in the same (15 mL) and cooled solution of the above reaction mixture.TMSCl (1.1 mL, 8.6 mmol) was added over 45 min and stirred at 0 °C for 30 min. Then benzoyl chloride (0.3 mL, 2.6 mmol) was added over 15 min, and the solution was stirred at room temperature for 2 h. Then ammonia solution (1.8 mL, in 9 mL of water) was added slowly at 0 °C and stirred for 30 min. The reaction mixture was allowed to warm to room temperature and stirred for another 16 h. After evaporation of solvent, the residual was chromatographed over silica gel (2.5−4.5% MeOH in DCM, v/v) to give **45a** as an off-white solid (0.35 g, 52%). R_f 0.4 (10% MeOH in DCM, v/v). ^{1}H NMR (600 MHz, $CDCl_3$): δ 8.58 (1H, s, H2), 8.51 (1H, s, H8), 7.96 (2H, d, J = 7.2 Hz, Ar−H), 7.53 (1H, t, J = 7.8 Hz, Ar−H), 7.40−7.48 (2H, m, Ar−H), 6.10 (1H, s, H1′), 4.51 (1H, s, H3′), 3.74 (1H, d, J = 12.6 Hz, H5″), 3.69 (1H, d, J = 12.6 Hz, H5′), 2.68−2.80 (1H, m, H7′), 2.53 (1H, d, J = 3 Hz, H2′), 1.95 (1H, t, J = 12 Hz, H6″), 1.24 (3H, d, J = 7.2 Hz, CH_3), 0.98 (1H, dd, J = 4.8 and 12.6 Hz, H6′). ^{13}C NMR (150.9 MHz, $CDCl_3$): δ 166.2 (PhC═O), 152.1 (C2), 150.8 (C4), 148.8 (C6), 141.8 (C8), 133.3 (Ar−C), 132.8 (Ar−C), 128.7 (Ar−C), 128 (Ar−C), 122.9 (C5), 90.8 (C4′), 83.0 (C1′), 72.5 (C3′), 59.5 (C5′), 50.4 (C2′), 36.6 (C6′), 28.8 (C7′), 15.6 (CH_3). MALDI-TOF m/z $[M + H]^+$ calcd for $C_{20}H_{22}N_5O_4$ 396.167, found 396.163.

(1*R*,3*R*,4*R*,5*R*,7*S*)-3-(*N*^{6}-Benzoyladenin-9-yl)-1-(4,4′-dimethoxytrityloxy)methyl-5-methyl-7-hydroxyl-2-oxa-bicyclo[2.2.1]-heptane (48a). Compound **45a** (0.5 g, 1.26 mmol) was coevaporated twice with dry pyridine (100 mL) and suspended in the same (100 mL). 4,4′-Dimethoxytrityl chloride (1.27 g, 3.78 mmol) was added and stirred for 16 h at rt. The reaction mixture was quenched with saturated aqueous $NaHCO_3$ and extracted three times with DCM. The organic layer was dried and evaporated, and the crude compound was chromatographed over silica gel (1% pyridine/methanol in DCM, v/v) to give **48a** (0.55 g, 80%) as yellow foam. R_f 0.40 (10% methanol in DCM, v/v). ^{1}H NMR (400 MHz, $CDCl_3$): δ 9.02 (1H, s, NH-Bz), 8.79 (1H, s, H2), 8.41 (1H, s, H8), 8.02 (2H, d, J = 8.72 Hz, Ar−H), 7.60−7.70 (4H, m, Ar−H), 7.44 (2H, d, J = 7.6 Hz, Ar−H), 7.30−7.35 (6H, m, Ar−H), 6.84 (4H, d, J = 8.72 Hz, Ar−H), 6.23 (1H, s, H1′), 4.38 (1H, s, H3′), 3.78 (6H, s, Ar-OMe), 3.56 (1H, d, J = 10.7 Hz, H5″), 3.36 (1H, d, J = 10.8 Hz, H5′), 2.65−2.90 (2H, m, H2′ and H7′), 2.12 (1H, d, J = 10.8 Hz, H6″), 1.36 (3H, d, J = 6.9 Hz, CH_3), 1.26 (1H, dd, J = 5.0 and 12.9 Hz, H6′). ^{13}C NMR (100.6 MHz, $CDCl_3$): δ 164.7 (COPh), 158.5 (Ar−C), 152.5 (C2), 150.6 (C4), 149.0 (C6), 144.4 (Ar−C), 141.2 (C8), 135.6 (Ar−C), 133.7 (Ar−C), 132.6 (Ar−C), 129.0 (Ar−C), 128.9 (Ar−C), 128.8 (Ar−C), 128.2 (Ar−C), 128.0 (Ar−C), 127.9 (Ar−C), 127.8 (Ar−C), 127.0 (Ar−C), 123.4 (C5), 113.2 (Ar−C), 88.8 (C4′), 86.5 (DMTr-C), 83.2 (C1′), 74.5 (C3′), 61.5 (C5′), 55.2 (DMTr-OMe), 50.4 (C2′), 37.3 (C6′), 28.6 (C7′), 15.6 (CH_3). MALDI-TOF m/z $[M + H]^+$ calcd for $C_{41}H_{40}N_5O_6$ 698.298, found 698.301.

(1*R*,3*R*,4*R*,5*R*,7*S*)-3-(*N*^{6}-Benzoyladenin-9-yl)-7-(2-cyanoethoxy-diisopropylamino-phosphinoxy)-1-(4,4′-dimethoxytrityloxy)-methyl-5-methyl-2-oxa-bicyclo[2.2.1]heptane (49a). Compound **48a** (0.950 g, 1.36 mmol) was dissolved in 45 mL of dry DCM, and DIPEA (1.18 mL, 6.80 mmol) was added at 0 °C followed by 2-cyanoethyl *N*,*N*-diisopropylphosphoramidochloridite (0.605 mL, 2.72 mmol). The reaction was stirred for 24 h at room temperature. Reaction was quenched by the addition of 0.1 mL of methanol and aqueous $NaHCO_3$ under cooling conditions and extracted twice (25 mL) with DCM. The organic phase was dried and evaporated. The obtained crude compound was purified by precipitation in *n*-hexane, to give **49a** (1.0 g, 81%) as a mixture of two isomers. ^{31}P NMR (161.97 MHz, $CDCl_3$): 149.38, 149.19. LC-MS m/z $[M + H]^+$ calcd for $C_{50}H_{57}N_7O_7P$ 898.40, found 898.30.

9-[4-*C*-Allyl-3,5-di-*O*-benzyl-2-*O*-acetyl-β-D-ribofuranosyl]-*N*^{2}-Acetyl-*O*^{6}-diphenylcarbamoyl-guanine (38b). *N*,*O*-Bis-(trimethylsilyl)acetamide (BSA) (32.0 mL, 131.6 mmol) was added to a stirred suspension of *O*^{6}-diphenylcarbamoyl-*N*^{2}-acetylguanine (13.6 g, 36.2 mmol) in dried 1,2-dichloroethane (164 mL). Stirring was continued under N_2 at 80 °C for 30 min. The clear solution was evaporated under reduced pressure. The residue was redissolved in dry toluene (100 mL). Trimethylsilyl triflate (TMSOTf) (7.74 mL, 42.8 mmol) and a solution of **37** (15.0 g, 32.9 mmol) in dried toluene (65 mL) were added. The solution was stirred at 80 °C for 1 h and was allowed to cool to rt. The reaction was quenched with saturated NH_4Cl solution, and volatiles were evaporated. The residual was redissolved in EtOAc, and the solution was washed with saturated aqueous $NaHCO_3$ solution. The organic layer was dried over anhydrous Na_2SO_4 and filtered. The filtrate was concentrated to dryness. The crude product obtained was purified by silica gel column chromatography (15−20% ethyl acetate in *n*-hexane, v/v) to give **38b** (15.4 g, 60%). ^{1}H NMR (400 MHz, $CDCl_3$): δ 8.24 (1H, s, H8), 7.89 (1H, s, NH), 7.40−7.25 (20H, m, Ar−H), 6.21 (1H, d, H1′, J = 5.0 Hz), 5.77−5.83 (2H, m, H7′, H2′), 5.07 (2H, d, J = 12 .4 Hz, H8′, H8″, 4.40−4.59 (5H, m, 2 × CH_2Ph, H3′), 3.60 (1H, d, J = 10.3 Hz, H5′), 3.39 (1H, d, J = 10.3 Hz, H5″), 2.65−2.71 (1H, dd, J = 6.3, 14.7 Hz, H6′), 2.53 (3H, s, 2-COCH_3), 2.32−2.39 (1H, m, H6″), 2.05 (3H, s, 2′-COCH_3). ^{13}C NMR (100.6 MHz, $CDCl_3$): δ 170.8 (NHC═O), 169.7 (2′-C═O), 156.0, 154.5 (C4), 152.1, 150.3 (C$\underline{O}$CONPh$_2$), 142.5 (C8), 141.7, 137.4, 137.2, 132.6 (C7′), 129.1, 128.5, 127.9, 127.8, 127.5, 126.4, 125.9, 120.9 (C5), 118.6 (C8′), 87.8 (C4′), 85.9 (C1′), 78.3 (C3′), 75.5 (C2′), 74.3 (O$\underline{C}$H$_2$Ph), 73.4 (O$\underline{C}$H$_2$Ph), 72.3 (C5′), 37.1 (C6′), 25.1 (NHCO$\underline{C}$H$_3$), 20.6 (OCO$\underline{C}$H$_3$). MALDI-TOF m/z $[M + H]^+$ calcd for $C_{44}H_{42}N_6O_8$ 783.315, found 783.312.

9-[4-*C*-Allyl-3,5-di-*O*-benzyl-β-D-ribofuranosyl]-*N*^{2}-acetyl-*O*^{6}-diphenylcarbamoyl-guanine (39b). A solution of compound **38b** (14 g, 17.9 mmol) in THF:water (2:1) (450 mL) was cooled to 0 °C and 2 N aqueous NaOH (34.4 mL, 4 equivalent) solution was added.

dx.doi.org/10.1021/jo200073q |*J. Org. Chem.* 2011, 76, 4408–4431

The reaction was stirred at 0 °C for 2 h. The reaction mixture was partitioned between diethyl ether and the aqueous layer. The organic layer was dried over anhydrous Na_2SO_4 and filtered. The filtrate was evaporated to dryness. The crude product was washed several times in 5% acetone/*n*-hexane mixture to yield white solid **39b** (11.6 g, 88%). ^{1}H NMR (400 MHz, $CDCl_3$): δ 8.15 (1H, s, H8), 8.03 (1H, s, NH), 7.17−7.42 (18H, m, Ar−H), 7.06 (2H, m, Ar−H), 5.95 (1H, d, *J* = 5.6 Hz, H1′), 5.78−5.81 (1H, m, H7′), 5.06−5.11 (3H, m, CH_2Ph and H8′), 4.92 (1H, bs, H2′), 4.67 (1H, d, *J* = 11.4 Hz, CH_2Ph), 4.33 (2H, s, CH_2Ph), 4.26 (1H, d, *J* = 5.6 Hz, H3′), 3.41 (2H, s, H5′and H5″), 2.68−2.70 (1H, m, H6′), 2.51−2.53 (1H, m, H6″), 2.32 (3H, bs, NHCOCH$_3$). ^{13}C NMR (100.6 MHz, $CDCl_3$): δ 169.4 (C═O), 155.7, 153.8 (C4), 151.1, 150.3 (CONPh$_2$), 142.7 (C8), 141.6, 138.0, 137.1, 133.0 (C7′), 129.1, 128.3, 128.2, 127.9, 127.6, 127.5, 121.1 (C5), 118.4 (C8′), 90.6 (C1′), 89.0 (C4′), 80.3 (C3′), 76.8 (C2′), 74.4 (OCH$_2$Ph), 73.4 (OCH$_2$Ph), 73.1 (C5′), 37.2 (C6′), 24.7 (NHCOCH$_3$). MALDI-TOF *m*/*z* [M + H]$^+$ calcd for $C_{42}H_{40}N_6O_7$ 741.304, found 741.308.

9-[4-*C*-Allyl-3,5-di-*O*-benzyl-2-*O*-phenoxythiocarbonyl-β-D-ribofuranosyl]-N^2-acetyl-O^6-diphenylcarbamoylguanine (40b). To a mixture of compound **39b** (10 g, 13.5 mmol) and 1-*N*-methylimidazole (2.25 mL, 28.4 mmol) in dry DCM (150 mL) was added phenyl chlorothionoformate (3.15 mL, 22.9 mmol), and the solution was stirred overnight at rt. The reaction was poured in saturated $NaHCO_3$ solution and extracted with DCM (3 × 250 mL). Combined organic phases were washed with saturated citric acid solution (3 × 50 mL), dried with Na_2SO_4, and filtered, and the filtrate was evaporated to dryness. The residual was purified over silica gel column chromatography (15−20% ethyl acetate in *n*-hexane, v/v) to yield **40b** as a white foam solid (9.79 g, 82%). ^{1}H NMR (400 MHz, $CDCl_3$): δ 8.24 (1H, s, H8), 7.88 (1H, s, NH), 7.25−7.41 (23H, m, Ar−H), 6.92−6.94 (2H, d, *J* = 7.8 Hz, Ar−H), 6.40 (1H, d, *J* = 5.8 Hz, H1′), 6.28 (1H, t, *J* = 5.6 Hz, H2′), 5.78−5.84 (1H, m, H7′), 5.08 (2H, d, *J* = 12.6 Hz, H8′, H8″), 4.71−4.76 (2H, m, OCH$_2$Ph and H3′), 4.60 (2H, d, *J* = 12.8 Hz, OCH$_2$Ph), 4.47 (1H, d, *J* = 11.7 Hz, OCH$_2$Ph), 3.64 (1H, d, *J* = 10.2 Hz, H5′), 3.47 (1H, d, *J* = 10.2 Hz, H5″), 2.67−2.73 (1H, dd, *J* = 6.1 and 14.5 Hz, H6′), 2.56 (3H, bs, NHCOCH$_3$), 2.40−2.44 (1H, m, H6″). ^{13}C NMR (100.6 MHz, $CDCl_3$): δ 194.0 (C═S), 170.9 (C═O), 156.1, 154.7 (C4), 153.2, 152.2, 150.3 (CONPh$_2$), 142.5 (C8), 141.7, 137.3, 137.1, 132.4 (C7′), 129.6, 129.1, 128.5, 128.1, 128.0, 127.9, 126.8, 125.7, 121.5 (C5), 118.8 (C8′), 88.1 (C4′), 85.0 (C1′), 83.5 (C2′), 77.9 (C3′), 74.8 (OCH$_2$Ph), 73.6 (OCH$_2$Ph), 72.9 (C5′), 37.2 (C6′), 25.3 (NHCOCH$_3$). MALDI-TOF *m*/*z* [M + H]$^+$ calcd for $C_{49}H_{44}N_6O_8S$ 877.303, found 877.304.

(1*R*,3*R*,4*R*,5*R*,7*S*)-3-(N^2-Acetyl-O^6-diphenylcarbamoylguanin-9-yl)-1-benzyloxymethyl-7-benzyloxy-5-methyl-2-oxa-bicyclco[2.2.1]heptane (42a), (1*R*,3*R*,4*R*,5*S*,7*S*)-3-(N^2-Acetyl-O^6-diphenylcarbamoylguanin-9-yl)-1-benzyloxymethyl-7-benzyloxy-5-methyl-2-oxa-bicyclco[2.2.1]heptane (42b), and (1*R*,5*R*,7*R*,8*S*)-7-(N^2-Acetyl-O^6-diphenylcarbamoylguanin-9-yl)-5-benzyloxymethyl-8-benzyloxy-6-oxa-bicyclo[3.2.1]-octane (42c). Compound **40b** (4.5 g, 5.13 mmol) was dissolved in anhydrous toluene (200 mL) to which N_2 gas was purged for half an hour. The reaction mixture was heated at 90 °C, and Bn_3SnH (1.38 mL in 10 mL of anhydrous toluene) and AIBN (0.84 g in 10 mL of anhydrous toluene) were added dropwise over 1.5 h and heated at 90 °C for another 30 min. Solvent was evaporated, and residue was applied to silica short column chromatography (15−25% EtOAc in *n*-hexane) to obtain compound **42a** as white foam (1.8 g, 48%). The remaining mixture was subjected to preparative HPLC separation to yield compound **42b** as a white foam solid (0.16 g, 4.3%) and white solid **42c** (0.150 g, 4%). Compound **42a**: ^{1}H NMR (400 MHz, $CDCl_3$): δ 8.39 (1H, s, H8), 7.97 (1H, s, NH), 7.14−7.43 (20H, m, Ar−H), 6.11 (1H, s, H1′), 4.62 (2H, q, *J* = 12.4 Hz, OCH$_2$Ph), 4.40 (2H, s, OCH$_2$Ph), 4.14 (1H, s, H3′), 3.72 (1H, d, *J* = 11.0 Hz, H5′), 3.64 (1H, d, *J* = 11.0, H5″), 2.59−2.67 (1H, m, H7′), 2.58 (1H, m, H2′), 2.55 (3H, s, NHCOCH$_3$), 2.03−2.11 (1H, m, H6″), 1.28 (3H, d, *J* = 7.2 Hz, 7′-CH_3), 1.22 (1H, m, H6′). ^{13}C NMR (100.6 MHz, $CDCl_3$): δ 171.0 (C═O), 155.9, 153.2 (C4), 151.8, 150.4 (CONPh$_2$), 142.4 (C8), 141.7, 137.8, 137.4, 129.1, 128.5, 128.2, 127.7, 127.5, 127.4, 126.0, 121.5 (C5), 88.7 (C4′), 83.4 (C1′), 80.1 (C3′), 73.4 (OCH$_2$Ph), 72.2 (OCH$_2$Ph), 67.1 (C5′), 48.3 (C2′), 37.5 (C6′), 28.5 (C7′), 25.1 (NHCOCH$_3$), 15.5 (7′-CH_3). MALDI-TOF *m*/*z* [M + H]$^+$ calcd for $C_{42}H_{40}N_6O_6$ 725.309, found 725.310. **42b**: ^{1}H NMR (400 MHz, $CDCl_3$): δ 8.41 (1H, s, H8), 8.17 (1H, s, NH), 7.14−7.60 (20H, m, 2 × Bn, DPC), 5.73 (1H, s, H1′), 4.64 (2H, q, *J* = 12.5 Hz, BnCH_2), 4.41 (2H, q, *J* = 12.0 Hz, BnCH_2), 4.05 (1H, s, H3′), 3.75 (2H, q, *J* = 11.0 Hz, H5′ and 5″), 2.61 (1H, bs, H2′), 2.55 (3H, s, Ac), 2.22 (1H, m, H7′), 2.02 (1H, dd, *J* = 8.5 Hz, H6″), 1.62 (1H, dd, *J* = 5.0 and 12.5 Hz, H6′), 1.27 (3H, d, *J* = 7.5 Hz, CH_3). ^{13}C NMR (100.6 MHz, $CDCl_3$): δ 171.1 (C═O), 155.8 (C6), 153.5 (C4), 151.8 (C2), 150.5 (OC(O)), 142.4 (C8), 141.8, 137.8, 137.3, 129.2, 128.5, 128.3, 127.9, 127.81, 127.8, 127.6, 127.5, 121.6 (C5), 88.6 (C4′), 88.2 (C1′), 79.8 (C3′), 73.4 (BnCH$_2$), 72.3 (BnCH$_2$), 67.0 (C5′), 48.1 (C2′), 38.8 (C6′), 33.7 (C7′), 25.1 (CH_3C(O)), 15.6 (CH_3). MALDI-TOF *m*/*z* [M + H]$^+$ calcd for $C_{42}H_{40}N_6O_6$ 725.309, found 725.313. **42c**: ^{1}H NMR (500 MHz, $CDCl_3$): δ 8.71 (1H, s, H8), 8.26 (1H, s, NH), 7.22−7.60 (20H, m, 2 × Bn, DPC), 6.16 (1H, s, H1′), 4.36−4.69 (4H, m, 2 × BnCH_2), 4.32 (1H, d, *J* = 5.0 Hz, H3′), 3.61 (1H, d, *J* = 11.0 Hz, H5″), 3.49 (1H, d, *J* = 11.0 Hz, H5′), 2.69 (1H, bs, H2′), 2.55 (3H, s, Ac), 2.01 (1H, m, H8″), 1.72−1.90 (4H, m, H6″, H7′, H7″ and H8′), 1.39 (1H, dd, H6′). ^{13}C NMR (125.8 MHz, $CDCl_3$): δ 171.1 (C═O), 155.8 (C6), 153.7 (C4), 151.8 (C2), 150.5 (OC(O)), 143.0 (C8), 141.7, 137.7, 137.6, 129.2, 128.6, 128.4, 127.9, 127.81, 127.8, 127.4, 121.5 (C5), 87.1 (C1′), 85.1 (C4′), 73.8 (C3′), 73.3 (BnCH$_2$), 72.0 (BnCH$_2$), 70.1 (C5′), 42.8 (C2′), 26.7 (C6′), 25.1 (CH_3C(O)), 21.1 (C8′), 17.8 (C7′). MALDI-TOF *m*/*z* [M + H]$^+$ calcd for $C_{42}H_{40}N_6O_6$ 725.309, found 725.310.

(1*R*,3*R*,4*R*,5*R*,7*S*)-3-(N^2-Acetylguanin-9-yl)-1-benzyloxymethyl-7-benzyloxy-5-methyl-2-oxa-bicyclco[2.2.1]heptane (42a′). A solution of **42a** (2.75 g, 3.78 mmol) in acetic acid (75 mL) was warmed at 55 °C with constant stirring for 12 h followed by stirring at rt overnight. The volatiles were evaporated under reduced pressure to give brownish oil. The residue was diluted with EtOAc (50 mL). To this mixture was added water (50 mL), and subsequently sonication led to white precipitate formation, which was filtered. The precipitate was washed with EtOAc/hexane (1:1) (150 mL), and residual solid was dissolved in DCM (50 mL). The organic layer was dried over Na_2SO_4 and filtered. The filtrate was concentrated to dryness to obtain white solid **42a′** (1.25 g, 62%). ^{1}H NMR (400 MHz, $CDCl_3$): δ 11.92 (1H, bs, NH), 8.81 (1H, bs, NH), 8.00 (1H, s, H8), 7.17−7.32 (10H, m, Ar−H), 5.90 (1H, s, H1′), 4.63 (1H, d, *J* = 12.2 Hz, OCH$_2$Ph), 4.55 (1H, d, *J* = 12.2 Hz, OCH$_2$Ph), 4.42 (2H, s, OCH$_2$Ph), 4.19 (1H, s, H3′), 3.70 (1H, d, *J* = 11.3 Hz, H5′), 3.63 (1H, d, H5″), 2.67 (1H, m, H7′), 2.53 (1H, d, *J* = 5.5 Hz, H2′), 2.27 (3H, s, NHCOCH$_3$), 2.03−2.11 (1H, m, H6″), 1.23 (4H, d, *J* = 8.2 Hz, 7′-CH_3 and H6′). ^{13}C NMR (100.6 MHz, $CDCl_3$): δ 173.0 (C═O), 156.0 (C6), 147.6 (C4), 147.3 (C2), 137.7, 137.43 (C8), 137.35, 128.3, 127.7, 121.1 (C5), 88.5 (C4′), 82.9 (C1′), 79.8 (C3′), 73.3 (OCH$_2$Ph), 71.8 (OCH$_2$Ph), 67.5 (C5′), 48.3 (C2′), 37.4 (C6′), 28.5 (C7′), 24.3 (NHCOCH$_3$), 15.3 (7′-CH_3). MALDI-TOF *m*/*z* [M + H]$^+$ calcd for $C_{29}H_{31}N_5O_5$ 530.241, found 530.244.

(1*R*,3*R*,4*R*,5*R*,7*S*)-3-(N^2-Acetylguanin-9-yl)-7-hydroxyl-1-hydroxymethyl-5-methyl-2-oxa-bicyclco[2.2.1]heptane (45b). Compound **42a′** (0.775 g, 1.46 mmol) was dissolved in methanol (75 mL) to which N_2 gas was purged for half an hour. To the reaction mixture was added formic acid (0.575 mL, 14.6 mmol) and 20% $Pd(OH)_2$/C (0.630 g). The reaction mixture was heated to reflux for 2.5 h. The reaction mixture was filtered over a bed of Celite and washed with hot methanol several times. The crude product obtained was purified on a preparative thin layer chromatography plate to obtain white

yellow solid **45b** (0.3 g, 60%). ^{1}H NMR (400 MHz, DMSO-d_6): δ 12.00 (1H, bs, NH), 11.56 (1H, bs, NH), 8.11 (1H, s, H8), 5.89 (1H, s, H1′), 5.35 (1H, d, J = 3.3 Hz, 3′-OH), 4.88 (1H, t, J = 5.5 Hz, 5′-OH), 4.18 (1H, s, H3′), 3.59 (2H, m, H5′, H5″), 2.67 (1H, m, H7′), 2.43 (1H, d, J = 3.2 Hz, H2′), 2.17 (3H, s, NHCOC$\underline{H}_3$), 1.86−1.96 (1H, m, H6′), 1.22 (3H, d, J = 7.3 Hz, 7′-C$\underline{H}_3$), 0.97−1.01 (1H, m, H6″). ^{13}C NMR (100.6 MHz, $CDCl_3$): δ 173.1 (C═O), 154.4 (C6), 147.2 (C4), 147.0 (C2), 136.6 (C8), 120.2 (C5), 89.6 (C4′), 81.0 (C1′), 71.7 (C3′), 58.3 (C5′), 49.4 (C2′), 36.3 (C6′), 27.8 (C7′), 23.4 (NHCO$\underline{C}$H$_3$), 15.3 (7′-$\underline{C}$H$_3$). MALDI-TOF m/z $[M + H]^+$ calcd for $C_{15}H_{19}N_5O_5$ 350.147, found 350.151.

(1*R*,3*R*,4*R*,5*R*,7*S*)-3-(*N*^{2}-Acetylguanin-9-yl)-1-(4,4′-dimethoxytrityloxymethyl)-7-hydroxyl-5-methyl-2-oxa-bicylco[2.2.1]-heptane (48b). Compound **45b** (0.4 g, 1.14 mmol) was coevaporated twice with dry pyridine (25 mL) and suspended in the same (25 mL). 4,4′-Dimethoxytrityl chloride (1.16 g, 3.42 mmol) was added and stirred overnight at rt. The reaction was quenched with saturated aqueous $NaHCO_3$ and extracted with DCM (3 × 50 mL). The combined organic phase was dried and evaporated, and the residue was chromatographed over silica gel (1% pyridine/DCM/methanol, v/v) to give **48b** (0.6 g, 0.92 mmol, 80%) as yellow foam. R_f 0.3 (10% methanol in DCM, v/v). ^{1}H NMR (400 MHz, $CDCl_3$): δ 11.95 (1H, bs, NH), 9.3 (1H, s, NH), 8.00 (1H, s, H8), 7.12−7.42 (10H, m, Ar−H), 6.78 (3H, d, J = 8.8 Hz, Ar−H), 5.85 (1H, s, H1′), 4.39 (1H, s, H3′), 3.73 (6H, s, Trityl-OMe), 3.42 (1H, d, J = 10.6 Hz, H5′), 3.35 (1H, d, H5″), 2.66−2.67 (1H, m, H7′), 2.48 (1H, m, H2′), 2.21 (3H, s, NHCOC$\underline{H}_3$), 2.08−2.11 (1H, m, H6′), 1.24 (1H, m, H6″), 1.28 (3H, d, J = 7.2 Hz, 7′-C$\underline{H}_3$). ^{13}C NMR (100.6 MHz, $CDCl_3$): δ 172.4 (C═O), 158.4, 155.8 (C6), 147.3 (C4), 147.1 (C2), 144.7, 137.8, 137.5 (C8), 135.8, 135.7, 130.0, 128.9, 128.2, 128.1, 127.8, 126.8, 125.3, 121.1 (C5), 113.1, 88.8 (C4′), 86.2 (DMTr-C), 82.6 (C1′), 74.3 (C3′), 61.8 (C5′), 55.1 (OMe), 50.7 (C2′), 37.3 (C6′), 28.3 (C7′), 24.3 (NHCO$\underline{C}$H$_3$), 15.5 (7′-$\underline{C}$H$_3$). m/z $[M + H]^+$ calcd for $C_{36}H_{37}N_5O_7$ 652.27, found 652.20.

(1*R*,3*R*,4*R*,5*R*,7*S*)-3-(*N*^{2}-Acetylguanin-9-yl)-7-(2-cyanoethoxy-diisopropylamino-phosphinoxy)-1-(4,4′-dimethoxytrityloxy-methyl)-5-methyl-2-oxa-bicyclo[2.2.1]heptane (49b). Compound **48b** (0.4 g, 0.614 mmol) was dissolved in 22 mL of dry DCM, and DIPEA (0.534 mL, 3.07 mmol) was added at 0 °C followed by 2-cyanoethyl-*N*,*N*-diisopropylphosphoramidochloridite (0.273 mL, 1.23 mmol). The reaction was stirred overnight at rt. Methanol (0.5 mL) was added followed by aqueous saturated $NaHCO_3$ and extracted twice (25 mL) with dichloromethane. The organic phase was dried, evaporated, and chromatographed on silica gel (5% Et_3N/DCM v/v) to give **49b** (0.4 g, 77%) as a mixture of two isomers. ^{31}P NMR (161.97 MHz, $CDCl_3$): 149.57, 148.26. LC-MS m/z $[M + H]^+$ calcd for $C_{45}H_{55}N_7O_8P$ 852.38, found 852.305.

1-[4-*C*-Allyl-3,5-di-*O*-benzyl-2-*O*-acetyl-β-D-ribofuranosyl]-*N*^{4}-benzoyl-5-methylcytosine (38c). Acetic anhydride (35.3 mL, 343 mmol) and acetic acid (196.2 mL) were added to **36** (13.5 g, 32.9 mmol) and cooled, and triflic acid (0.28 mL) was added to it and stirred. After 30 min the reaction was quenched with cold saturated $NaHCO_3$ solution and extracted with ethyl acetate. The organic layer was washed with saturated $NaHCO_3$ until the aqueous layer is neutralized. The crude mixture was co-evaporated with dry CH_3CN (3 × 350 mL) and dissolved in the same. N^4-Benzoyl-5-methylcytosine (7.92 g, 34.4 mmol) and *N*,*O*-bis(trimethylsilyl)acetamide (15.3 mL, 85.2 mmol) were added to this solution and refluxed for 45 min until the suspension becomes a clear solution. This solution was cooled to 0 °C, and TMSOTf (5.72 mL, 23.2 mmol) was added dropwise and stirred overnight at rt. The organic solvent was evaporated and quenched with saturated NH_4Cl solution and extracted with ethyl acetate (3 × 250 mL). The organic layer was dried, evaporated, and chromatographed over silica gel eluting with 10% ethyl acetate in hexane (v/v) to give **38c** as a white foam solid (15.0 g, 80%). R_f 0.6 (30% ethyl acetate in hexane, v/v).^{1}H NMR (600 MHz, $CDCl_3$): δ 13.22 (1H, s, NH, D_2O exchangeable), 8.30 (2H, d, J = 7.2 Hz, Ar- H), 7.69 (1H, s, H6), 7.48−7.53 (1H, m, Ar−H), 7.28−7.42 (12H, m, Ar−H), 6.3 (1H, d, J = 4.0 Hz, H1′), 5.74−5.92 (1H, m, H7′), 5.45 (1H, t, J = 5.4 Hz, H2′), 5.07−5.12 (2H, m, H8′), 4.65 (1H, d, J = 11.4 Hz, CH_2−Ph), 4.42−4.61 (3H, m, CH_2−Ph), 4.38 (1H, d, J = 6.0 Hz, H3′), 3.72 (1H, d, J = 10.2 Hz, H5″), 3.41 (1H, d, J = 10.2 Hz, H5′), 2.68 (1H, dd, J = 6.0 and 14.4 Hz, H6″), 2.35 (1H, dd, J = 8.4 Hz, H6′), 2.10 (3H, s, $COCH_3$), 1.60 (3H, s, Cy-CH_3). ^{13}C NMR (150.9 MHz, $CDCl_3$): δ 179.6 (C$\underline{O}$Bz), 170.0 (C$\underline{O}$CH$_3$), 159.6 (C4), 148.1 (C2), 137.5 (Ar−C), 137.3 (Ar−C), 137.2 (Ar−C), 136.9 (C6), 132.6 (C7′), 132.4 (Ar−C), 127.6−129.9 (Ar−C), 118.7 (C8′), 112.2 (C5), 87.3 (C4′), 86.5 (C1′), 77.6 (C3′), 75.4 (C2′), 74.4 (OBn), 73.7 (OBn), 73.0 (C5′), 37.3 (C6′), 20.7 (CO$\underline{C}$H$_3$), 13.1 (Cy-$\underline{C}$H$_3$). MALDI-TOF m/z of $[M + H]^+$ calcd for $C_{36}H_{38}N_3O_7$ 624.271, found 624.270.

1-[4-*C*-Allyl-3,5-di-*O*-benzyl-β-D-ribofuranosyl]-*N*^{4}-benzoyl-5-methylcytosine (39c). Compound **38c** (13 g, 20.8 mmol) was dissolved in 50 mL of THF and cooled to 0 °C. To this cold solution (2.7 g, 67.5 mmol) NaOH in 15 mL of water was added dropwise over 15 min at the same temperature, and the mixture was stirred for 2 h at rt. The reaction mixture was quenched with water and extracted with EtOAc (200 mL). The organic layer was dried over Na_2SO_4, concentrated under reduced pressure, and chromatographed over silica gel eluting with 15% ethyl acetate in hexane (v/v) to give **39c** as a white foam solid (11.5 g, 95%). R_f 0.3 (30% ethyl acetate in hexane, v/v). ^{1}H NMR (600 MHz, $CDCl_3$): δ 13.25 (1H, s, NH, D_2O exchangeable), 8.27 (2H, m, Ar−H), 7.62 (1H, s, H6), 7.25−7.58 (13H, m, Ar−H), 6.01 (1H, d, J = 5.4 Hz, H1′), 5.81−5.89 (1H, m, H7′), 5.09−5.12 (2H, m, H8′), 4.70 (2H, q, J = 11.4 Hz, CH_2−Ph), 4.53 (2H, q, J = 11.4 Hz, CH_2−Ph), 4.39 (1H, dd, J = 6.0 and 12.5 Hz, H2′), 4.20 (1H, d, J = 6.0 Hz, H3′), 3.60 (1H, d, J = 10.2 Hz, H5″), 3.45 (1H, d, J = 10.2 Hz, H5′), 2.99 (1H, d, J = 7.2 Hz, O*H*, D_2O exchangeable), 2.75 (1H, dd, J = 6.0 and 14.4 Hz, H6″), 2.34 (1H, dd, J = 8.4 and 15.0 Hz, H6′), 1.73 (3H, s, CH_3). ^{13}C NMR (150.9 MHz, $CDCl_3$): δ 179.5 (C$\underline{O}$Bz), 159.6 (C4), 148.5 (C2), 137.4 (Ar−C), 137.3 (Ar−C), 137.1 (Ar−C), 137.0 (C6), 132.7 (C7′), 132.4 (Ar−C), 129.9 (Ar−C), 128.7 (Ar−C), 128.7 (Ar−C), 128.6 (Ar−C), 128.4 (Ar−C), 128.2 (Ar−C), 128.1 (Ar−C), 128.0 (Ar−C), 127.6 (Ar−C), 118.7 (C8′), 111.9 (C5), 89.4 (C1′), 87.2 (C4′), 79.6 (C3′), 75.4 (C2′), 74.8 (OBn), 73.8 (OBn), 73.7 (C5′), 37.5 (C6′), 13.2 (Cy-$\underline{C}$H$_3$). MALDI-TOF m/z $[M + H]^+$ calcd for $C_{34}H_{36}N_3O_6$ 582.261, found 582.263.

9-[4-*C*-Allyl-3,5-di-*O*-benzyl-2-*O*-phenoxythiocarbonyl-β-D-ribofuranosyl]-*N*^{4}-benzoyl-5-methyl-cytosine (40c). Compound **39c** (10.5 g, 18.07 mmol) was dissolved in 230 mL of dry DCM and cooled to 0 °C, and to this precooled solution was added 1-methylimidazole (2.85 mL, 36.0 mmol) and stirred for 20 min at the same temperature. To this mixture was added dropwise phenyl chlorothionoformate (3.49 mL, 25.3 mmol), and the reaction was stirred for 1.5 h at rt. The reaction was quenched with saturated solution of $NaHCO_3$ and extracted with DCM. The organic layer was dried over Na_2SO_4, concentrated, and chromatographed over silica gel eluting with 10% ethyl acetate in hexane (v/v) to give **40c** as a white foam (11.9 g, 92%). R_f 0.5 (20% ethyl acetate in hexane, v/v). ^{1}H NMR (600 MHz, $CDCl_3$): δ 13.1 (1H, s, N*H*, D_2O exchangeable), 8.28 (2H, d, J = 7.8 Hz, Ar−H), 7.70 (1H, s, H6), 7.27−7.58 (15H, m, Ar−H), 7.0 (2H, d, J = 7.8 Hz, Ar−H), 6.48 (1H, d, J = 6.0 Hz, H1′), 6.0 (1H, dd, J = 5.4 Hz, H2′), 5.79−5.86 (1H, m, H7′), 5.08−5.12 (2H, m, H8′), 4.79 (1H, d, J = 10.8 Hz, OBn), 4.50−4.57 (4H, m, CH_2−Ph and H3′), 3.75 (1H, d, J = 10.2 Hz, H5″), 3.50 (1H, d, J = 10.2 Hz, H5′), 2.68 (1H, dd, J = 6.0 and 15.0 Hz, H6″), 2.37 (1H, dd, J = 7.8 and 14.4 Hz, H6′), 1.67 (3H, s, Cy-CH_3). ^{13}C NMR (150.9 MHz, $CDCl_3$): δ 194.5 (C═S), 179.4 (C$\underline{O}$Bz), 159.5 (C4), 153.5 (Ar−C), 148.0 (C2C$\underline{O}$), 137.3 (Ar−C), 137.2 (Ar−C), 137.16 (Ar−C), 137.1 (C6), 132.5 (C7′), 132.45 (Ar−C), 130.0 (Ar−C), 129.6 (Ar−C), 129.4 (Ar−C), 128.7 (Ar−C), 128.5 (Ar−C), 128.2 (Ar−C), 128.15 (Ar−C), 128.1 (Ar−C), 127.9

dx.doi.org/10.1021/jo200073q |*J. Org. Chem.* 2011, 76, 4408–4431

(Ar−C), 126.8 (Ar−C), 121.7 (Ar−C), 118.9 (C8′), 112.3 (C5), 87.5 (C4′), 85.8 (C1′), 83.3 (C2′), 77.9 (C3′), 75.0 (OBn), 73.8 (OBn), 73.7 (C5′), 37.5 (C6′), 13.1 (Cy-CH_3). MALDI-TOF m/z $[M + H]^+$ calcd for $C_{41}H_{40}N_3O_7S$ 718.259, found 718.261.

(1*R*,3*R*,4*R*,5*R*,7*S*)-3-(N^4-Benzoyl-5-methylcytosin-1-yl)-1-benzyloxy-7-benzyloxymethyl-5-methyl-2-oxa-bicylco[2.2.1]-heptane (43a), (1*R*,3*R*,4*R*,5*S*,7*S*)-3-(N^4-Benzoyl-5-methylcytosin-1-yl)-1-benzyloxy-7-benzyloxymethyl-5-methyl-2-oxa-bicylco[2.2.1]heptane (43b), and (1*R*,5*R*7*R*,8*S*)-7-(N^4-Benzoyl-5-methylcytosin-1-yl)-8-benzyloxy-5-benzyloxmethyl-6-oxa-bicyclo[3.2.1]octane (43c). Compound **40c** (11.0 g, 15.34 mmol) was dissolved in 600 mL of dry toluene and purged with dry nitrogen for 30 min. Bu_3SnH (4.16 mL, 15.34 mmol) was dissolved in 50 mL of dry toluene, and half of this solution was added dropwise to refluxing solution over 30 min. AIBN (3.0 g, 18.29 mmol) was dissolved in 50 mL of dry toluene and added to the above solution dropwise, and simultaneously was added the remaining solution of Bu_3SnH over 60−70 min. After 60 min of reflux, the solution was cooled, CCl_4 (100 mL) added, and the mixture stirred for 20 min. A solution of iodine in DCM was added to the above solution until a faint coloration persisted, and then solvent was evaporated. The solid obtained was taken up in EtOAc. The organic layer was dried, evaporated, and chromatographed over silica gel (10−12% EtOAc in hexane, v/v) to give a mixture of **43a**/**b**/**c** as a white foam (5.2 g, 60%, ^{1}H NMR showed that **43a:43b:43c** = 79:12:9). R_f 0.6 (30% ethyl acetate in hexane, v/v). Compound **43a**: ^{1}H NMR (500 MHz, $CDCl_3$): δ 13.4 (1H, s, NH, D_2O exchangeable), 8.31 (2H, m, Ar−H), 7.93 (1H, s, H6), 7.24−7.53 (13H, m, Ar−H), 5.81 (1H, s, H1′), 4.43−4.63 (4H, m, 2 × OBn), 4.03 (1H, s, H3′), 3.82 (1H, d, J = 11.0 Hz, H5″), 3.72 (1H, d, J = 10.5 Hz, H5′), 2.66 (1H, m, H2′), 2.60−2.66 (1H, m, H7′), 2.08 (1H, dd, J = 11.0 and 12.0 Hz, H6″), 1.71 (3H, s, Cy-CH_3), 1.28 (3H, d, J = 7.5 Hz, 7′CH_3), 1.18 (1H, dd, J = 4.5 and 12.5 Hz, H6′). ^{13}C NMR (125.8 MHz, $CDCl_3$): δ 179.5 (BzCO), 160.2 (C4), 147.5 (C2), 138.1 (C6), 137.8 (Ar−C), 137.5 (Ar−C), 137.4 (Ar−C), 132.3 (Ar−C), 129.8 (Ar−C), 128.6 (Ar−C), 128.4 (Ar−C), 128.3 (Ar−C), 128.1 (Ar−C), 128.0 (Ar−C), 127.9 (Ar−C), 127.8 (Ar−C), 127.5 (Ar−C), 110.4 (C5), 89.1 (C4′), 84.6 (C1′), 78.6 (C3′), 73.7 (OBn), 71.9 (OBn), 67.6 (C5′), 47.6 (C2′), 37.7 (C6′), 28.8 (C7′), 15.5 (7′CH_3), 13.2 (Cy-CH_3). MALDI-TOF m/z $[M + H]^+$ calcd for $C_{34}H_{36}N_3O_5$ 566.266, found 566.269. **43b**: ^{1}H NMR (500 MHz, $CDCl_3$): δ 13.4 (1H, s, NH, D_2O exchangeable), 8.30−8.32 (2H, m, Ar−H), 7.92 (1H, s, H6), 7.25−7.53 (13H, m, Ar−H), 5.43 (1H, s, H1′), 4.57−4.63 (3H, m, OBn), 4.23−4.45 (1H, d, J = 11.5 Hz, OBn), 3.93 (1H, s, H3′), 3.86 (1H, d, J = 11.0 Hz, H5″), 3.80 (1H, d, J = 11.0 Hz, H5′), 2.60−2.61 (1H, m, H2′), 2.16−2.21 (1H, m, H7′), 1.95 (1H, dd, J = 9.0 and 12.5 Hz, H6″), 1.67 (3H, s, Cy-CH_3), 1.60 (1H, dd, J = 5.5 and 12.5 Hz, H6′), 1.25 (3H, d, J = 7.5 Hz, 7′CH_3). ^{13}C NMR (125.8 MHz, $CDCl_3$): δ 179.4 (BzCO), 160.1 (C4), 147.7 (C2), 137.9 (C6), 137.8 (Ar−C), 137.3 (Ar−C), 132.3 (Ar−C), 129.8 (Ar−C), 129.0 (Ar−C), 128.6 (Ar−C), 128.5 (Ar−C), 128.4 (Ar−C), 128.1 (Ar−C), 128.0 (Ar−C), 127.9 (Ar−C), 127.7 (Ar−C), 127.5 (Ar−C), 110.2 (C5), 89.1 (C1′), 88.9 (C4′), 78.2 (C3′), 73.7 (OBn), 72.0 (OBn), 67.5 (C5′), 47.7 (C2′), 38.6 (C6′), 33.6 (C7′), 20.1 (7′CH_3), 13.1 (Cy-CH_3). MALDI-TOF m/z $[M + H]^+$ calcd for $C_{34}H_{36}N_3O_5$ 566.266, found 566.267. **43c**: ^{1}H NMR (600 MHz, $CDCl_3$): δ 13.45 (1H, s, NH, D_2O exchangeable), 8.30 (2H, m, Ar−H), 8.28 (1H, s, H6), 7.29−7.52 (13H, m, Ar−H), 5.87 (1H, s, H1′), 4.60−4.62 (2H, m, OBn), 4.55 (1H, d, J = 11.4 Hz, OBn), 4.45 (1H, d, J = 12.0 Hz, OBn), 4.17 (1H, d, J = 4.8 Hz, H3′), 3.71 (1H, d, J = 10.8 Hz, H5″), 3.58 (1H, d, J = 10.2 Hz, H5′), 2.65 (1H, m, H2′), 1.91−1.97 (1H, m, H8″), 1.84−1.89 (1H, m, H6″), 1.77−1.79 (1H, m, H8′), 1.69−1.75 (2H, m, H7′/7″), 1.59 (3H, s, Cy-CH_3), 1.35−1.37 (1H, m, H6′). ^{13}C NMR (150.9 MHz, $CDCl_3$): δ 179.5 (BzCO), 160.2 (C4), 147.9 (C2), 138.3 (C6), 137.8 (Ar−C), 137.5 (Ar−C), 137.4 (Ar−C), 132.2 (Ar−C), 129.8 (Ar−C), 128.6 (Ar−C), 128.5 (Ar−C), 128.1 (Ar−C), 128.07 (Ar−C), 127.9 (Ar−C), 127.89 (Ar−C), 127.5 (Ar−C), 127.4 (Ar−C), 127.3 (Ar−C), 110.3 (C5), 88.0 (C1′), 85.6 (C4′), 73.6 (OBn), 72.9 (C3′), 71.7 (OBn), 70.7 (C5′), 42.7 (C2′), 26.8 (C6′), 20.7 (C8′), 17.7 (C7′), 12.9 (Cy-CH_3). MALDI-TOF m/z $[M + H]^+$ calcd for $C_{34}H_{36}N_3O_5$ 566.266, found 566.264.

Isomeric Mixture of (1*R*,3*R*,4*R*,5*R*,7*S*)-7-Hydroxyl-1-hydroxymethyl-5-methyl-3-(5-methylcytosin-1-yl)-2-oxa-bicylco[2.2.1]-heptane (46a), (1*R*,3*R*,4*R*,5*S*,7*S*)-7-Hydroxyl-1-hydroxymethyl-5-methyl-3-(5-methylcytosin-1-yl)-2-oxa-bicylco[2.2.1]heptane (46b), and (1*R*,5*R*,7*R*,8*S*)-8-Hydroxyl-5-hydroxymethyl-7-(5-methylcytosin-1-yl)-6-oxa-bicyclo[3.2.1]octane (46c). A mixture of **43a**/**b**/**c** (3.5 g, 5.84 mmol) was dissolved in methanolic ammonia (100 mL) and stirred under a nitrogen atmosphere for 8 h at rt. The reaction mixture was concentrated under vacuum to get **43′** as off-white foam (2.5 g, 90%), R_f 0.2 (40% EtOAc in hexane, v/v). m/z of $[M + H]^+$ found 461.90, calculated mass of 461.23. To a solution of **43′** (2.0 g, 4.33 mmol) in methanol (200 mL) were added 20% $Pd(OH)_2/C$ (4.0 g) and ammonium formate (16.3 g, 258 mmol), and the mixture was heated at 60 °C for 16 h. After the reaction was finished as seen by TLC, the suspension was filtered through Celite, and $Pd(OH)_2/C$ was washed with (5 × 400 mL) methanol. The solvent was evaporated. The crude compound was chromatographed over silica gel eluting with 10% methanol in DCM (v/v) to give **46a**/**b**/**c** as a white foamy solid (0.833 g, 70%). R_f 0.13 (10% methanol in DCM, v/v). **46a** is the major product, and **46b** is the minor product. ^{1}H NMR (400 MHz, DMSO-d_6): δ 8.2 (0.09H, s, H6, Minor), 7.79−7.80 (1H, m, H6, Major), 7.2 (1H, s, NH, D_2O exchangeable), 6.7 (1H, s, N*H*, D_2O exchangeable), 5.55 (1H, s, H1′, Major), 5.02−5.2 (2.3H, m, H1′, Minor and OH, D_2O exchangeable), 3.8−3.98 (1H, m, H3′ Major and Minor), 3.52−3.74 (2H, m, H5′, H5″), 2.52−2.59 (1H, m, H7′, Major), 2.09−2.2 (1H, m, H2′ Major and Minor), 1.99 (0.5H, m, H7′ Minor), 1.80−1.90 (4.0H, m, Cy-CH_3 Major and Minor, H6″ Major), 1.71−1.75 (0.5H, m, H6″, Minor), 1.39 (0.3H, s, H6′, Minor), 1.13−1.22 (3.2H, m, 7′CH_3, Major and Minor), 0.90 (1H, dd, J = 4.5 and 12.2 Hz, H6′ Major). ^{13}C NMR (100.6 MHz, DMSO-d_6): δ 164.9 (C2), 154.4, 154.3 (C4, Major), 138.1, 137.9 (C6), 99.1, 98.9 (C5), 89.5 (C4′), 87.5 (C1′, Minor), 82.4 (C1′, Major), 70.0, 69.8 (C3′), 58.1, 57.8 (C5′), 49.3 (C2′), 36.3 (C6′, Minor), 36.4 (C6′, Major), 33.1 (C7′, Minor), 27.8 (C7′, Major), 20.1 (7′CH_3, Minor), 15.1 (7′CH_3, Major), 13.0 (Cy-CH_3 Major and Minor). MALDI-TOF m/z $[M + H]^+$ calcd for $C_{13}H_{20}N_3O_4$ 282.146, found 282.150.

Isomeric Mixture of (1*R*,3*R*,4*R*,5*R*,7*S*)-3-(N^4-Benzoyl-5-methylcytosin-1-yl)-7-hydroxyl-1-hydroxymethyl-5-methyl-2-oxa-bicylco[2.2.1]heptane (47a), (1*R*,3*R*,4*R*,5*S*,7*S*)-3-(N^4-Benzoyl-5-methylcytosin-1-yl)-7-hydroxyl-1-hydroxymethyl-5-methyl-2-oxa-bicylco[2.2.1]heptane (47b), and (1*R*,5*R*,7*R*,-8*S*)-7-(N^4-Benzoyl-5-methylcytosin-1-yl)-8-hydroxyl-5-hydroxymethyl-6-oxa-bicyclo[3.2.1]octane (47c). A mixture of compound **46a**/**b**/**c** (2.5 g, 8.89 mmol) was evaporated twice with dry pyridine and suspended in the same (15 mL). To this solution benzoic anhydride (4.0 g, 17.6 mmol) was added and stirred at rt overnight and diluted with EtOH (32.5 mL), and 2 M NaOH (50 mL) was added. After stirring for 1 h, AcOH (6.25 mL) was added to the solution, and the solvent was removed under reduced pressure. The residue was purified by chromatography over silica gel, 40% ethyl acetate in hexane (v/v) to give three portions: **47a**/**47b**/**47c** as a mixture (2.7 g, 77%), **47a** (0.600 g, 13%), and **47b** (0.080 g, 10%). R_f 0.4 (60% EtOAc in hexane, v/v). **47a**: ^{1}H NMR (600 MHz, DMSO-d_6) δ 13.3 (1H, s, NH, D_2O exchangeable), 8.2 (3H, bs, Ar−H), 7.58−7.60 (1H, m, Ar−H), 7.48−7.54 (2H, m, Ar−H), 5.67 (1H, s, H1′), 5.32 (1H, s, OH, D_2O exchangeable), 5.18 (1H, t, J = 4.8 Hz, OH, D_2O exchangeable), 4.00 (1H, s, H3′), 3.67 (1H, dd, J = 4.8 and 12.6 Hz, H5″), 3.60 (1H, dd, J = 4.8 and 12.0 Hz, H5′), 2.57−2.65 (1H, m, H7′), 2.31 (1H, d, J = 3.0 Hz, H2′), 2.0 (3H, s, Cy-CH_3), 1.91 (1H, t, J = 11.4 Hz, H6″), 1.17 (3H, d, J = 7.2 Hz, 7′CH_3),

0.95 (1H, dd, J = 4.2 and 12.6 Hz, H6′). ^{13}C NMR (150.9 MHz, DMSO-d_6) δ 139.3 (C6), 132.9 (Ar−C), 132.3 (Ar−C), 129.2 (Ar−C), 128.2 (Ar−C), 90.7 (C4′), 83.9 (C1′), 70.4 (C3′), 58.2 (C5′), 49.5 (C2′), 36.6 (C6′), 28.2 (C7′), 15.4 (7′CH_3), 13.4 (Cy-CH_3). m/z $[M+H]^+$ calcd for $C_{20}H_{24}N_3O_5$ 384.16, found 384.00. **47b**: ^{1}H NMR (500 MHz, DMSO-d_6) δ 13.3 (1H, s, N*H*, D_2O exchangeable), 8.23 (1H, s, H6), 8.02−8.31 (2H, m, Ar−H), 7.54−7.62 (1H, m, Ar−H), 7.42−7.51 (2H, m, Ar−H), 5.33 (1H, d, J = 3.0 Hz, 3′-O*H*, D_2O exchangeable), 5.29 (1H, s, H1′), 5.22 (1H, bt, 5′-O*H*, D_2O exchangeable), 3.95 (1H, s, H3′), 3.70 (2H, s, H5′ and H5″), 2.28 (1H, s, H2′), 1.21 (3H, d, J = 7.0 Hz, 7′CH_3), 2.06 (1H, m, H7′), 2.01 (3H, s, Cy-CH_3), 1.76 (1H, dd, J = 9.0 and 12.0 Hz, H6″), 1.44 (1H, dd, J = 5.0 and 12.5 Hz, H6′). ^{13}C NMR (125.8 MHz, DMSO-d_6) δ 139.6 (C6), 132.3 (Ar−C), 129.1 (Ar−C), 128.6 (Ar−C), 128.2 (Ar−C), 107.9 (C5), 90.7 (C4′), 88.4 (C1′), 70.1 (C3′), 58.6 (C5′), 49.4 (C2′), 37.6 (C6′), 33.3 (C7′), 20.4 (7′CH_3), 13.3 (Cy-CH_3). MALDI-TOF m/z $[M + H]^+$ calcd for $C_{20}H_{24}N_3O_5$ 386.172, found 386.171.

Isomeric Mixture of (1*R*,3*R*,4*R*,5*R*,7*S*)-3-(N^4-Benzoyl-5-methylcytosin-1-yl)-1-(4,4′-dimethoxytrityloxymethyl)-7-hydroxyl-5-methyl-2-oxa-bicylco[2.2.1]heptane (50a), (1*R*,3*R*,4*R*,5*S*,7*S*)-3-(N^4-Benzoyl-5-methylcytosin-1-yl)-1-(4,4′-dimethoxytrityloxymethyl)-7-hydroxyl-5-methyl-2-oxa-bicylco-[2.2.1]heptane (50b), and (1*R*,5*R*,7*R*,8*S*)-7-(N^4-Benzoyl-5-methylcytosin-1-yl)-5-(4,4′-dimethoxytrityloxymethyl)-8-hydroxyl-6-oxa-bicyclo[3.2.1]octane (50c). A mixture of **47a/b/c** (0.190 g, 0.493 mmol) was evaporated twice with dry pyridine and suspended in the same (10 mL). 4,4′-Dimethoxytrityl chloride (0.256 g, 0.757 mmol) was added and stirred overnight at rt. The reaction was quenched with saturated aqueous $NaHCO_3$ and extracted with DCM (3 × 10 mL). The organic layer was dried and evaporated, and chromatographic separation over silica gel (1% pyridine/EtOAc in hexane, v/v) furnished **50a/50b/50c** (0.180 g, 53%) as yellow foam. R_f 0.60 (40% EtOAc/Hexane, v/v). **50a** is the major product, and **50b** is the minor product. ^{1}H NMR (400 MHz, $CDCl_3$): δ 13.4 (1H, s, NH, D_2O exchangeable), 8.30 (2H, d, J = 7.3 Hz, Ar−H), 8.0 (1H, s, H6), 7.21−7.54 (14H, m, Ar−H), 6.86 (4H, dd, J = 3.5 and 5.4 Hz, Ar−H), 5.7 (1H, s, H1′ Major), 5.36 (0.27H, s, H1′ Minor), 4.28 (1.2H, s, H3′ Major and Minor), 3.79 (7H, s, OMe, Major and Minor), 3.60−3.63 (1.4H, m, H5′ Major and Minor), 3.37 (0.38H, d, J = 11.1 Hz, H5′, Minor), 3.30 (1H, d, J = 11.1 Hz, H5′), 2.64 (1H, bs, H7′ Major), 2.54 (1H, d, J = 3.0 Hz, H2′ Major), 2.18 (0.3H, m, H7′ Minor), 2.46 (0.3H, s, H2′ Minor), 1.89−1.99 (1.4H, m, H6″ Major and Minor), 1.76 (3H, s, Cy-CH_3), 1.71 (1H, s, Cy-CH_3, Minor), 1.47 (0.5H, dd, J = 4.7 and 11.3 Hz, H6′, Minor), 1.21−1.26 (4H, m, 7′CH_3), 1.11 (1H, d, J = 4.9 and 12.8 Hz, H6′ Major). ^{13}C NMR (100.6 MHz, $CDCl_3$): δ 179.1 (COBz), 160.2 (C4), 158.7 (Ar−C), 144.6 (C2), 137.5, 137.3 (C6), 135.6 (Ar−C), 135.5 (Ar−C), 132.3 (Ar−C), 130.1 (Ar−C), 129.8 (Ar−C), 128.1 (Ar−C), 127.1 (Ar−C), 113.3 (Ar−C), 110.6 (C5), 89.7 (C4′), 86.7 (DMTr-C), 84.5 (C1′), 72.9 (C3′), 61.0 (C5′), 55.3 (OMe), 50.2 (C2′), 37.4 (C6′), 28.5 (C7′), 15.4 (7′CH_3), 13.5 (Cy-CH_3). m/z $[M + H]^+$ calcd for $C_{41}H_{42}N_3O_7$ 688.30, found 688.20.

(1*R*,3*R*,4*R*,5*R*,7*S*)-3-(N^4-Benzoyl-5-methylcytosin-1-yl)-7-(2-cyanoethoxy-diisopropylamino-phosphinoxy)-1-(4,4′-dimethoxytrityloxymethyl)-5-methyl-2-oxa-bicylco[2.2.1]heptane (51a), (1*R*,3*R*,4*R*,5*S*,7*S*)-3-(N^4-Benzoyl-5-methylcytosin-1-yl)-7-(2-cyanoethoxy-diisopropylamino-phosphinoxy)-1-(4,4′-dimethoxytrityloxymethyl)-5-methyl-2-oxa-bicylco[2.2.1]heptane (51b), and (1*R*,5*R*,7*R*,8*S*)-7-(N^4-Benzoyl-5-methylcytosin-1-yl)-8-(2-cyanoethoxy-diisopropylamino-phosphinoxy)-5-(4,4′-dimethoxytrityloxymethyl)-6-oxa-bicyclo[3.2.1]octane (51c). Compound **50a/b/c** (0.250 g, 0.364 mmol) was dissolved in 10 mL of dry DCM, and DIPEA (0.32 mL, 1.802 mmol) was added at 0 °C followed by 2-cynoethyl-*N*,*N*-diisopropylphosphoramidochloridite (0.16 mL, 0.728 mmol). The reaction was stirred at rt for 2 h. Methanol (0.3 mL) was added followed by aqueous saturated $NaHCO_3$ and extracted with dry DCM (2 × 15 mL). The organic phase was dried and washed with hexane:DCM (4:1) 3 times to give **51a/b/c** (0.250 g, 75%) as a mixture of six isomers as a white solid. R_f 0.75 (40% EtOAc/Hexane, v/v). ^{31}P NMR (161.97 MHz, $CDCl_3$): δ 150.20, 150.04, 149.46, 149.22, 148.94, 148.80. LC-MS m/z $[M + H]^+$ calcd for $C_{50}H_{59}N_5O_8P$ 888.41, found 888.50.

Oligonucleotide Synthesis and Purification. All AONs were synthesized using an automated DNA/RNA synthesizer based on phosphoramidite chemistry. For native A, G, and C building blocks, fast deprotecting phosphoramidites (Ac for C, *i*Pr-Pac for G, Pac for A) were used. Standard DNA synthesis reagents and cycle were used except that 0.25 M 5-[3,5-bis(trifluoromethyl)phenyl]-1*H*-tetrazole (activator 42) was used as the activator and Tac_2O as the cap A. For incorporation of modified nucleotides, extended coupling time (10 min compared to 25 s for native nucleotides) was used. The deprotections were carried out in 33% aqueous NH_3 for 10 h at 55 °C. After deprotection, all crude oligos were purified by denaturing PAGE (20% polyacrylamide with 7 M urea), extracted with 0.3 M NaOAc, and desalted with a C-18 reverse phase cartridge to give AONs in >99% purity, and correct masses have been obtained by MALDI-TOF mass spectroscopy for each of them.

RNA was also synthesized by a solid-supported phosphoramidite approach based on the 2′-O-TEM strategy.

UV Melting Experiments. Determination of the T_m of the AON/RNA hybrids or AON/DNA duplex was carried out in the following buffer: 60 mM Tris-HCl (pH 7.5), 60 mM KCl, 0.8 mM $MgCl_2$. Absorbance was monitored at 260 nm in the temperature range from 20 to 95 °C using an UV spectrophotometer equipped with a Peltier temperature programmer with the heating rate of 1 °C/min. Prior to measurements, the samples (1 μM of AON and 1 μM cDNA or RNA mixture) were preannealed by heating to 80 °C for 5 min followed by slow cooling to 21 °C and 30 min equilibration at this temperature. The value of T_m is the average of two or three independent measurements. If the error of the first two measurements is > ± 0.3 °C, the third measurement was carried out to check if the error is indeed within ±0.3 °C; otherwise, it is repeated.

^{32}P Labeling of Oligonucleotides. The oligoribonucleotides and oligodeoxyribonucleotides were 5′-end labeled with ^{32}P using T4 polynucleotide kinase, [γ-^{32}P]ATP, and the standard protocol. Labeled AONs and the target RNA were purified by a Nucleotide Removal Kit, and specific activities were measured using a counter.

SVPDE Degradation of AONs 1−8. Stability of the AONs toward 3′-exonucleases was tested using phosphodiesterase I from *Crotalus adamanteus*. All reactions were performed at 3 μM DNA concentration (5′-end ^{32}P labeled with specific activity 80 000 cpm) in 100 mM Tris-HCl (pH 8.0) and 15 mM $MgCl_2$ at 21 °C. An exonuclease concentration of 6.7 ng/μL was used for digestion of oligonucleotides. Total reaction volume was 30 μL. Aliquots (3 μL) were taken at proper time points and quenched by addition of stop solution (4 μL) [containing 0.05 M EDTA, 0.05% (w/v) bromophenol blue, and 0.05% (w/v) xylene cyanole in 80% formamide]. Reaction progress was monitored by 20% denaturing (7 M urea) PAGE and autoradiography.

Michaelis−Menten Kinetics of SVPDE Digestion of AONs 9−16. AONs (concentration varied from 1 to 100 μM) and SVPDE (for AONs **9**−**12**, 0.000055 unit SVPDE used; for AONs **13**−**16**, 0.0000825 unit SVPDE used) were mixed in a buffer containing100 mM Tris-HCl, pH 8.0, 100 mM NaCl, and 15 mM $MgCl_2$ at 21 °C, with a total reaction volume of 30 μL. Aliquots (3 μL) were taken at proper time points and quenched by addition of stop solution (4 μL) [containing 0.05 M EDTA, 0.05% (w/v) bromophenol blue, and 0.05% (w/v) xylene cyanole in 80% formamide]. Reaction progress was monitored by 20% denaturing (7 M urea) PAGE and autoradiography. The total percentage of integrated AON was plotted against time points to give the initial velocities (v_0) of the reactions (see Supporting Information part IV). Values of the kinetic parameters (K_M and V_{max}) in

this method were determined directly from v_0 versus concentration of substrate (C_0) plots (see Supporting Information part IV) using a correlation Program, where the correlation equation was $y = ax/(b + x)$, where $a = V_{max}$ and $b = K_M$. k_{cat} was obtained from this equation: $k_{cat} = V_{max}/E_0$, where E_0 corresponds to the concentration of enzyme used in the reaction. All values are averages and standard deviations of 3−4 independent experiments.

Stability Studies in Human Blood Serum. AONs at 2 μM concentration (5′-end ^{32}P labeled with specific activity 80 000 cpm) were incubated in 10 μL of human blood serum (male AB) at 21 °C (total reaction volume was 36 μL). Aliquots (3 μL) were taken at proper time points and quenched with 4 μL of stop solution [containing 0.05 M EDTA, 0.05% (w/v) bromophenol blue, and 0.05% (w/v) xylene cyanole in 80% formamide], resolved in 20% polyacrylamide denaturing (7 M urea) gel electrophoresis, and visualized by autoradiography.

RNase H Digestion Assay. Target 0.1 μM RNA (specific activity 80 000 cpm) and AON (2 μM) were incubated in a buffer containing 20 mM Tris-HCl (pH 7.5), 20 mM KCl, 10 mM $MgCl_2$, 0.1 mM EDTA, and 0.1 mM DTT at 21 °C in the presence of 0.08 U *E. coli* RNase H1. Prior to the addition of the enzyme, reaction components were preannealed in the reaction buffer by heating at 80 °C for 5 min followed by slow cooling to 21 °C and 30 min equilibration at this temperature. Total reaction volume was 30 μL. Aliquots of 3 μL were removed after 5, 10, 15, 30, and 60 min, and the reactions were terminated by mixing with stop solution [containing 0.05 M EDTA, 0.05% (w/v) bromophenol blue, and 0.05% (w/v) xylene cyanole in 80% formamide]. The samples were subjected to 20% 7 M urea PAGE and visualized by autoradiography. Pseudofirst-order reaction rates could be obtained by fitting the digestion curves to single-exponential decay functions.

■ ASSOCIATED CONTENT

Supporting Information. NMR data for all the new synthesized compounds; PAGE pictures as well as degradation curves, showing the cleavage kinetics of AONs by SVPDE, blood serum. This material is available free of charge via the Internet at http://pubs.acs.org.

■ AUTHOR INFORMATION

Corresponding Author

*Phone: +46-18-4714577. Fax: +46-18-554495. E-mail: jyoti@boc.uu.se.

Author Contributions

[§]RamShankar Upadhayaya, Sachin Gangadhar Deshpande, and Qing Li have contributed equally to this work.

■ ACKNOWLEDGMENT

Generous financial support from the Swedish Natural Science Research Council (Vetenskapsrådet), the Swedish Foundation for Strategic Research (Stiftelsen för Strategisk Forskning), the EU-FP6 funded RIGHT project (Project no. LSHB-CT-2004-005276), and Department of Science and Technology, India (Grant no.VII-PRDSF/109/05-06), is gratefully acknowledged. Authors also acknowledge the contribution of Yogesh Walunj, Sachin Borude, and Tushar Gawali for scaleup of some of the reactions.

■ ABBREVIATIONS

Bn, (benzyl); Ac, (acetyl); TMSOTf, (trimethylsilyl triflate); THF, (tetrahydrofuran); AIBN, [2,2′-azobis(2-methyl-propionitrile)]; DCM, dichloromethane; DMTr, (4,4′-dimethoxytrityl); DIPEA, (diisopropylethylamine); EtOAc, (ethyl acetate)

■ REFERENCES

(1) (a) Castanotto, D.; Rossi, J. J. *Nature* **2009**, *457*, 426–433. (b) Kurreck, J. *Eur. J. Biochem.* **2003**, *270*, 1628–1644.

(2) (a) Watts, J. K.; Deleavey, G. F.; Damha, M. J. *Drug Discovery Today* **2008**, *13*, 842–855. (b) Cook, P. D. In *Current Protocols in Nucleic Acid Chemistry*; John Wiley & Sons, Inc.: New York, 2000. (c) Shukla, S.; Sumaria, C. S.; Pradeepkumar, P. I. *ChemMedChem* **2010**, *5*, 328–349.

(3) (a) Obika, S.; Nanbu, D.; Hari, Y.; Morio, K.-I.; In, Y.; Ishida, T.; Imanishi, T. *Tetrahedron Lett.* **1997**, *38*, 8735–8738. (b) Obika, S.; Nanbu, D.; Hari, Y.; Andoh, J.-I.; Morio, K.-I.; Doi, T.; Imanishi, T. *Tetrahedron Lett.* **1998**, *39*, 5401–5404. (c) Imanishi, T.; Obika, S. *J. Synth. Org. Chem. Jpn.* **1999**, *57*, 969–980. (d) Singh, S. K.; Nielsen, P.; Koshkin, A. A.; Wengel, J. *Chem. Commun.* **1998**, 455–456. (e) Koshkin, A. A.; Singh, S. K.; Nielsen, P.; Rajwanshi, V. K.; Kumar, R.; Meldgaard, M.; Olsen, C. E.; Wengel, J. *Tetrahedron* **1998**, *54*, 3607–3630. (f) Singh, S. K.; Wengel, J. *Chem. Commun.* **1998**, 1247–1248. (g) Koshkin, A. A.; Rajwanshi, V. K.; Wengel, J. *Tetrahedron Lett.* **1998**, *39*, 4381–4384. (h) Koshkin, A. A.; Nielsen, P.; Meldgaard, M.; Rajwanshi, V. K.; Singh, S. K.; Wengel, J. *J. Am. Chem. Soc.* **1998**, *120*, 13252–13253.

(4) (a) Kumar, S.; Hansen, M. H.; Albaek, N.; Steffansen, S. I.; Peterson, M.; Nielsen, P. *J. Org. Chem.* **2009**, *74*, 6756–6769. (b) Plashkevych, O.; Chatterjee, S.; Honcharenko, D.; Pathmasiri, W.; Chattopadhayaya, J. *J. Org. Chem.* **2007**, *72*, 4716–4726 and references cited therein.

(5) Petersen, M.; Nielsen, C. B.; Nielsen, K. E.; Jensen, G. A.; Bondensgaard, K.; Singh, S. K.; Rajwanshi, V. K.; Koshkin, A. A.; Dahl, B. M.; Wengel, J.; Jacobsen, J. P. *J. Mol. Recognit.* **2000**, *13*, 44–53.

(6) (a) Kaur, H.; Babu, B. R.; Maiti, S. *Chem. Rev.* **2007**, *107*, 4642–4697. (b) Zhou, C.; Chattopadhyaya, J. *Curr. Opin. Drug. Discovery Dev.* **2009**, *12*, 876–898.

(7) (a) Singh, S. K.; Kumar, R.; Wengel, J. *J. Org. Chem.* **1998**, *63* (26), 10035–10039. (b) Seth, P. P.; Vasquez, G.; Allerson, C. A.; Berdeja, A.; Gaus, H.; Kinberger, G. A.; Prakash, T. P.; Migawa, M. T.; Bhat, B.; Swayze, E. E. *J. Org. Chem.* **2010**, *75*, 1569–1581. (c) Prakash, T. P.; Siwkowski, A.; Allerson, C. R.; Migawa, M. T.; Lee, S.; Gaus, H. J.; Black, C.; Seth, P. P.; Swayze, E. E.; Bhat, B. *J. Med. Chem.* **2010**, *53*, 1636–1650. (d) Hari, Y.; Obika, S.; Ohnishi, R.; Eguchi, K.; Osaki, T.; Ohishi, H.; Imanishi, T. *Bioorg. Med. Chem.* **2006**, *14*, 1029–1038. (e) Rahman, S. M. A.; Seki, S.; Obika, S.; Yoshikawa, H.; Miyashita, K.; Imanishi, T. *J. Am. Chem. Soc.* **2008**, *130*, 4886–4896.

(8) Pradeepkumar, P. I.; Cheruku, P.; Plashkevych, O.; Acharya, P.; Gohil, S.; Chattopadhyaya, J. *J. Am. Chem. Soc.* **2004**, *126*, 11484–11499.

(9) Honcharenko, D.; Varghese, O. P.; Plashkevych, O.; Barman, J.; Chattopadhyaya, J. *J. Org. Chem.* **2006**, *71*, 299–314.

(10) Koizumi, M. *Curr. Opin. Mol. Ther.* **2006**, *8*, 144–149.

(11) Morita, K.; Takagi, M.; Hasegawa, C.; Kaneko, M.; Tsutsumi, S.; Sone, J.; Ishikawa, T.; Imanishi, T.; Koizumi, M. *Bioorg. Med. Chem.* **2003**, *11*, 2211–2226.

(12) Varghese, O. P.; Barman, J.; Pathmasiri, W.; Plashkevych, O.; Honcharenko, D.; Chattopadhyaya, J. *J. Am. Chem. Soc.* **2006**, *128*, 15173–15187.

(13) (a) Albæk, N.; Petersen, M.; Nielsen, P. *J. Org. Chem.* **2006**, *71*, 7731–7740. (b) Enderlin, G.; Nielsen, P. *J. Org. Chem.* **2008**, *73*, 6891–6894.

(14) (a) Srivastava, P.; Barman, J.; Pathmasiri, W.; Plashkevych, O.; Wenska, M.; Chattopadhyaya, J. *J. Am. Chem. Soc.* **2007**, *129*, 8362–8379. (b) Zhou, C.; Plashkevych, O.; Chattopadhyaya, J. *Org. Biomol. Chem.* **2008**, *6*, 4627–4633. (c) Zhou, C.; Liu, Y.; Andaloussi, M.; Badgujar, N.; Plashkevych, O.; Chattopadhyaya, J. *J. Org. Chem.* **2009**, *74*, 118–134. (d) Xu, J. F.; Liu, Y.; Dupouy, C.; Chattopadhyaya, J. *J. Org. Chem.* **2009**, *74*, 6534–6554. (e) Li, Q.; Yuan, F.; Zhou, C.; Plashkevych, O.; Chattopadhyaya, J. *J. Org. Chem.* **2010**, *75*, 6122–6140. (f) Liu, Y.; Xu, J.; Karimiahmadabadi, M.; Zhou, C.; Chattopadhyaya, J. *J. Org. Chem.* **2010**, *75*, 7112–7128. (g) Zhou, C.; Plashkevych, O.;

Chattopadhyaya, J. *J. Org. Chem.* **2009**, *74*, 3248–3265. (h) Seth, P. P.; Allerson, C. R.; Berdeja, A.; Siwkowski, A.; Pallan, P. S.; Gaus, H.; Prakash, T. P.; Watt, A. T.; Egli, M.; Swayze, E. E. *J. Am. Chem. Soc.* **2010**, *132*, 14942–14950.

(15) Zhou, C.; Chattopadhyaya, J. *J. Org. Chem.* **2010**, *75*, 2341–2349.

(16) Wenska, M.; Honcharenko, D.; Pathmasiri, W.; Chattopadhyaya, J. *Heterocycles* **2007**, *73*, 303–324.

(17) Robins, M. J.; Zou, R.; Guo, Z.; Wnuk, S. F. *J. Org. Chem.* **1996**, *61*, 9207–9212.

(18) Buchini, S.; Leumann, C. J. *Eur. J. Org. Chem.* **2006**, 3152–3168.

(19) (a) Julia, M. *Acc. Chem. Res.* **1971**, *4*, 386–392. (b) Beckwith, A. L. J. *Tetrahedron* **1981**, *37*, 3073–3100. (c) Beckwith, A. L. J. *Chem. Soc. Rev.* **1993**, 143–151.

(20) Ti, G. S.; Gaffney, B. L.; Jones, R. A. *J. Am. Chem. Soc.* **1982**, *104*, 1316–1319.

(21) Foldesi, A.; Yamakage, S.-I.; Nilson, F. P. R.; Maltseva, T. V.; Chattopadhyaya, J. *Nucleic Acids Res.* **1996**, *24*, 1187–1194.

(22) Debart, F.; Rayner, B.; Degols, G.; Imbach, J.—L. *Nucleic Acids Res.* **1992**, *20*, 1193–1200.

(23) Foldesi, A.; Trifonova, A.; Dinya, Z.; Chattopadhyaya, J. *Tetrahedron Lett.* **1999**, *40*, 7283–7284.

(24) (a) Koshkin, A. A.; Fensholdt, J.; Pfundheller, H. M.; Lomholt, C. *J. Org. Chem.* **2001**, *66*, 8504–8512. (b) Kumar, T. S.; Kumar, P.; Sharma, P. K.; Hrdlicka, P. J. *Tetrahedron Lett.* **2008**, *49*, 7168–7170.

(25) Dörper, T.; Winnacker, E.-L. *Nucleic Acids Res.* **1983**, *11*, 2575–2584.

(26) The cause for the formation of P(V) was described; for oxidation of P(III) to P(V) phosphoramidite under aqueous acidic conditions is known: Sanghvi, Y. S.; Guo, Z.; Pfundheller, H. M.; Converso, A. *Org. Process Res. Dev.* **2005**, *9*, 730–737.

(27) Beaucage, S. L.; Caruthers, M. H. In *Current Protocols in Nucleic Acid Chemistry*; John Wiley & Sons: New York, 2003.

(28) Shaw, J. P.; Kent, K.; Bird, J.; Fishback, J.; Froehler, B. *Nucleic Acids Res.* **1991**, *19*, 747–750.

(29) Miyashita, K; Abdur Rahman, S. M.; Seki, S.; Obika, S.; Imanishi, T. *Chem. Commun.* **2007**, 3765–3767.

(30) (a) Razzell, W. E.; Khorana, H. G. *J. Biol. Chem.* **1959**, *234*, 2105–2117. (b) Razzell, W. E. *Methods Enzymol.* **1963**, *6*, 236–258.

(31) Pradeepkumar, P. I.; Chattopadhyaya, J. *J. Chem. Soc., Perkin Trans.* **2001**, *2*, 2074–2083.

(32) Why are AON/RNA duplexes more stable than their AON/DNA counterpart? The total free energy of stabilization of a duplex has at least two major components besides hydration: the free-energy of base-pairing and free-energy of stacking. This interdependency of stacking and hydrogen bonding has been shown to play a key role in the total free-energy of stabilization of AON/DNA versus AON/RNA versus RNA/RNA duplexes. In most isosequential duplexes (T is switched for U in RNA), the order of stability follows the following order RNA/RNA > DNA/RNA > DNA/DNA because of variable contribution of stacking versus hydrogen bonding. The dissection of the relative energetic contributions from the free-energy of base-pairing and free-energy of stacking to the total free-energy of stabilization allows us to understand the differences in the intrinsic nature of the electrostatic forces that are responsible for the self-assembly of the heteroduplexes (AON/RNA) compared to homoduplexes (DNA/DNA versus RNA/RNA). The pK_a differences between the monomeric nucleotides in both 2′-deoxy (dN) and ribo (rN) series (N = A/G/C/T/U), as the model donor and acceptor (in which stacking is completely eliminated), gives: Acharya, P.; Cheruku, P.; Chatterjee, S.; Acharya, S.; Chattopadhyaya, J. *J. Am. Chem. Soc.* **2004**, *126*, 2862. The strength of base-pairing energies in different homo- and heteroduplexes:Chatterjee, S.; Pathmasiri, W.; Chattopadhyaya, J. *Org. Biomol. Chem.* **2005**, *3*, 3911–3915. The high correlation of ΔG°_{37} of the helix stability and the sum of ΔpK_a values in a duplex ($\Sigma\Delta pK_a$) give a powerful tool to separate base-pairing contribution of RNA/RNA over DNA/RNA and DNA/DNA ([ΔG^{o}_{bp}]RR-DD) from the free energy of the total helix stability ([ΔG^{o}_{bp}]RR-DD or DR). The study shows that the stability of DNA/RNA duplexes is dependent on the number of 5-Me(T) stacking interactions, and the contribution of the base-pairing strength is relatively smaller. In contradistinction, RNA/RNA duplexes are more stable than DNA/DNA duplexes because of larger energy gain from the base-pairing in the former compared to the latter:Acharya, P.; Cheruku, P.; Chatterjee, S.; Acharya, S.; Chattopadhyaya, J. *J. Am. Chem. Soc.* **2004**, *126*, 2862. A comparison of these two linear plots ([ΔG^{o}_{bp}]RR-DD/DR versus [$\Delta G^{o}_{stacking}$]RR-DD/DR as a function of % A-T/U bp content) with opposite slope shows that with the increasing content of A-T base pairs the stability of the DNA/DNA duplex weakens over the corresponding DNA/RNA or RNA/RNA duplexes ([$\Delta G^{o}_{stacking}$]RR-DD/RD), while the strength of stacking ([$\Delta G^{o}_{stacking}$]RR-DD/RD) of A-T rich DNA/DNA sequence increases in comparison with A-U rich sequence in RNA/RNA duplexes. This increased stacking contribution from T compared to U, in DNA/DNA, followed by DNA/RNA over RNA/RNA duplex, comes from favorable electrostatic CH/σ^* interaction between the 5-methyl group of T with the nearest-neighbor A in the AT-rich sequence.

(33) Recently, carba-LNA has been studied against various biological targets to evaluate the true potential of carba-LNA (cLNA). Corey et al. tested the broad spectrum of modified antisense oligonucleotides (AON) targeted to patient-derived fibroblast cell lines GM04281 (69 CAG repeat mutant allele), GM04717 (41 CAG repeat mutant allele), and GM04719 (44 CAG repeat mutant allele) involving a direct comparison of IC_{50}s (based on protein and RNA analysis) within LNA and cLNA modified AON (with phosphodiester backbone). Corey; *Biochemistry* **2010**, *49*, 10166–10178. These studies clearly showed that cLNA is better than any other modification including LNA in terms of selective inhibition of HTT. Quantification of Western blots upon dose response revealed that LNA modified AON potencies range from IC_{50} values of 27−40 nM and selectivities of inhibition for mutant versus wild-type HTT by as much as >3.7-fold, whereas cLNA modified AONs were found to be more potent compared to their LNA counterpart with IC_{50} of 15 nM and >6.6-fold selectivity over the wild-type. Corey et al. also studied phosphorothioate modified AONs and revealed that cLNA-PS and LNA-PS achieved comparable potent and selective inhibition of HTT. Another study involved carba-LNA (cLNA) and LNA modified siRNAs for silencing the target HIV-1 TAR RNA employing a standard single cell replication model using HEK 293T cells:Suman; *Med. Chem. Commun.* **2011**, *2*, 206. This study clearly showed that cLNA modified siRNAs (IC_{50} = 0.54 nM) have 2-fold lower IC_{50} values than that of their LNA counterpart (IC_{50} = 1.13 nM) with 3−4-fold higher stability in human blood serum. Apart from these studies, Punit et al. have studied the potential of carba-LNA (cLNA) versus LNA and methylene-cLNA in cell culture (brain endothelial cells using electroporation) and animal experiments (subchronic dosing schedule in mice).Punit; *J. Am. Chem. Soc.* **2010**, *132*, 14942–14950. These experiments revealed that carba-LNA were slightly less potent compared to LNA and methylene-cLNA AONs. This particular set of experiments differs in their delivery techniques as the electroporation method has been used to assist the delivery of AONs, while the earlier studies have used lipid-based transfacting agents; therefore, the transfection efficiency of carba-LNA modified AONs should be studied in light of the electroporation technique. It is also clear that it is not always straightforward to understand why particularly modified AONs are more effective than others, especially with such a wide variety of targets and experimental conditions. A number of factors can complicate an oligonucleotide's ability to reach its target RNA and inhibit gene expression. Simple explanations might include poor transfection or release from endosomes after cell entry and cellular uptake.